

Gravitational Causality and the Self-Stress of Photons

Brando Bellazzini^{1,2}, Giulia Isabella^{1,3},
Matthew Lewandowski⁴, and Francesco Sgarlata⁵

¹ *Institut de Physique Théorique, Université Paris Saclay, CEA, CNRS, F-91191 Gif-sur-Yvette, France*

² *CERN, Theoretical Physics Department, Geneva, Switzerland*

³ *Université Paris-Saclay, CNRS/IN2P3, IJCLab, 91405 Orsay, France*

⁴ *Department of Physics and Astronomy, Northwestern University, Evanston, IL 60208, USA*

⁵ *Department of Physics, LEPP, Cornell University, Ithaca, NY 14853, USA*

Abstract

We study causality in gravitational systems beyond the classical limit. Using on-shell methods, we consider the one-loop corrections from charged particles to the photon energy-momentum tensor —the self-stress— that controls the quantum interaction between two on-shell photons and one off-shell graviton. The self-stress determines in turn the phase shift and time delay in the scattering of photons against a spectator particle of any spin in the eikonal regime. We show that the sign of the β -function associated to the running gauge coupling is related to the sign of time delay at small impact parameter. Our results show that, at first post-Minkowskian order, asymptotic causality, where the time delay experienced by any particle must be positive, is respected quantum mechanically. Contrasted with asymptotic causality, we explore a local notion of causality, where the time delay is longer than the one of gravitons, which is seemingly violated by quantum effects.

Contents

1	The Photon Self-Stress	4
1.1	Self-Stress at One Loop	5
1.2	Non-Minimal Couplings and Higgs/Graviton Mixing	9
1.3	Trace Anomaly and the Running Coupling	10
1.4	IR-Divergences and Sudakov Double-Logarithms	12
2	The Phase Shift	13
2.1	Amplitudes in the Eikonal Limit	13
2.2	Computation of the Phase Shift	14
2.2.1	The Large b Limit	15
2.2.2	The Small b Limit for Loops of Scalars and Fermions	16
2.2.3	The Small b Limit for Loops of Vectors	17
3	Causality	17
3.1	Time Delay	17
3.2	Asymptotic Causality	19
3.3	Bulk Causality	20
4	Conclusions	21
A	Conventions	22
B	Free Energy-Momentum Tensors	23
C	Higgs/Graviton Mixing	23
D	Explicit Form Factors at One Loop	24
E	Off-Shell Vertices	26

Introduction

Causality is a cornerstone of relativistic quantum field theory (QFT), with one of its most profound implications being the existence of anti-particles. Furthermore, causality has important implications for properties of scattering amplitudes in flat space, such as analyticity in the complex plane of Mandelstam variables. In combination with unitarity, causality enforces non-trivial consistency conditions on effective field theories (EFTs) that emerge at low-energy from underlying causal and unitary QFTs, often in the form of “positivity constraints” on the EFT’s Wilson coefficients that enter in 4-point scattering, see e.g. [1].

The notion of causality in the presence of gravity is certainly more subtle because the spacetime metric that defines the causal structure is itself subject to quantum fluctuations. Moreover, quantum fluctuations give rise to different light-cones for the various species of particles.

A fundamental step in understanding the role of causality in gravity has been taken in [2], where the properties of 3-point vertices involving at least one graviton have been linked to the tree level classical corrections of the time delay that particles experience in eikonal scattering. Requiring positive time delay over all range of impact parameters provides thus non-trivial causality constraints on the 3-point functions.

In this work we are interested in gravitational causality beyond the classical limit and study the first non-trivial quantum effects. The question that we have in mind is the following: what notion of causality is respected —quantum-mechanically— once gravity generates spacetime backgrounds? When quantum loops are taken into account, is the theory causal with respect to a local light cone defined by the metric in the bulk of spacetime (“bulk causality”) or rather with respect to the asymptotic metric at infinity (“asymptotic causality”)?

We address these questions by studying eikonal scattering around flat spacetime perturbatively, where some spectator source weakly perturbs Minkowski space and generates a non-trivial scattering phase shift, hence a time delay or advance, for photons that are sent through such space. We focus in particular on the gauge one-loop corrections ($o(g^2/16\pi^2)$) to the time delay, while working to the lowest post-Minkowskian order $o(1/m_{\text{Pl}}^2)$, i.e. neglecting gravitational loop contributions.

The causal response of photons in a perturbed Minkowski space is extracted by calculating the self-stress (energy-momentum tensor) of photon pairs at one loop. We consider loops of charged states of massive scalars, fermions, and vectors, which is equivalent to the full one-loop correction to the 3-point function as predicted by the Standard Model. The self-stress is parametrized by three gravitational form factors $F_i(q^2)$, for $i = 1, 2, 3$ with q the momentum of the exchanged graviton, that correspond to 3-point functions with off-shell gravitons having a non-trivial momentum dependence that in turn affects the time delay in the eikonal scattering, see Fig. 1.

The detailed computation of the form factors is performed via on-shell methods (unitarity cuts, massive spinor-helicity formalism, and dispersion relations), which are computationally powerful and conceptually neat, avoiding the need to deal with gauge-dependent quantities to extract physical observables. For wavelengths of the exchanged graviton larger than the charged-particle Compton wavelength $1/m$ in the loop, we recover the classic results of [3] (extended to include spin-1 loops), from which the study of causality in the low-energy limit of quantum electrodynamics (QED) coupled to gravity originally started. At shorter graviton wavelengths, virtual particles can probe larger regions of spacetime. As a result, we show that the sign of the time delay at small impact parameters $b \ll 1/m$ is related to the sign of the QED β -function contribution from charged particles.

We find no asymptotic-causality violation for impact parameters larger than the length scale associated to the Landau pole (below which our calculations no longer apply) in spinorial and scalar

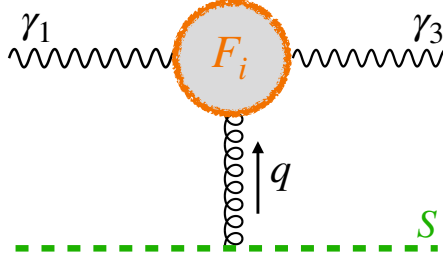


Figure 1: Type of diagram contributing to the time delay via the form factors F_i . Curly lines are graviton legs, wiggle lines represent photons, dashed lines are the spectators, and F_i are the form factors defined in Eq. (1.3).

QED. Loops of spin-1 W -bosons do not generate a Landau pole¹ and give in fact no asymptotic-causality violation because of Sudakov infrared (IR) divergences which exponentiate and suppress the form factor at large momentum transfer. Instead, and despite being classically valid, we find that bulk causality is not respected quantum mechanically, within our setup. We interpret these results as further evidence that in gravity only boundary data, such as asymptotic time delay, is meaningful quantum mechanically.

The remainder of this paper is organized as follows. In Sec. 1 we calculate the energy-momentum tensor at one loop in the Standard Model and study its properties, including the connection between the gravitational form factors, β -functions, and IR divergences. We also study the Higgs/graviton mixing that contributes to the form factors. In Sec. 2, we calculate the phase shift by taking the eikonal limit of the amplitudes in the relevant kinematic configuration and computing its Fourier transform to impact parameter space. Different limits of the integration are studied analytically at large and small impact parameter. Sec. 3 is devoted study the implications of the one-loop self-stress on the two notions of causality. Conclusions and future directions are discussed in Sec. 4.

1 The Photon Self-Stress

In this section we calculate the matrix element of a symmetric and conserved energy-momentum tensor $T_{\mu\nu}$ in flat spacetime

$$\langle 0|T_{\mu\nu}(x)|k'k\rangle = e^{-i(k+k')\cdot x}\langle 0|T_{\mu\nu}(0)|k'k\rangle, \quad T_{\mu\nu} = T_{\nu\mu} \quad \partial_\mu T^{\mu\nu} = 0 \quad (1.1)$$

between a pair of (identical) incoming massless spin-1 particle states, both taken on-shell,

$$k^2 = k'^2 = 0, \quad \epsilon \cdot k = \epsilon' \cdot k' = 0, \quad (1.2)$$

where the dot \cdot indicates Lorentz contraction with the Minkowski metric (see App. A for conventions), and $k^2 \equiv k \cdot k$. The ϵ and ϵ' are polarization vectors associated, up to a gauge choice, to k and k' respectively.² In analogy with low-energy quantum electrodynamics, we refer hereafter to these states as “photons,” although our analysis goes beyond real world QED to any massless spin-1 minimally coupled to gravity. By crossing symmetry, Eq. (1.1) determines as well the $\langle k'|T_{\mu\nu}(x)|k\rangle$ matrix element by the replacement $\epsilon' \rightarrow \epsilon'^*$ and $k' \rightarrow -k'$ in Eq. (1.3), which flips the helicity.

¹We are including Higgs bosons to make the theory renormalizable in the absence of gravity.

²The little-group index that labels the helicity of the particles is sometime left understood to avoid clutter of notation, but displayed whenever relevant.

After Fourier transforming (1.1) and factoring out a $(2\pi)^4 \delta^4(k + k' + q)$ from momentum conservation, the matrix element can be written as the sum of three conserved and gauge-invariant tensor structures multiplied by scalar form factors $F_i(t)$, for $i = 1, 2, 3$,

$$\begin{aligned} \langle 0 | T_{\mu\nu}(0) | k' k \rangle \mathcal{N} = & \langle 0 | T_{\mu\nu}(0) | k' k \rangle \Big|^\text{tree} \mathcal{N} F_1(t) \\ & + P_{\mu\nu}(q) [2(\epsilon' \cdot k)(\epsilon \cdot k') - q^2(\epsilon \cdot \epsilon')] F_2(t) \\ & + p_\mu p_\nu [2(\epsilon' \cdot k)(\epsilon \cdot k') - q^2(\epsilon \cdot \epsilon')] F_3(t) \end{aligned} \quad (1.3)$$

where we have defined

$$p \equiv k' - k, \quad q = -(k + k'), \quad t = q^2 = 2k \cdot k', \quad P_{\mu\nu}(q) = q_\mu q_\nu - \eta_{\mu\nu} q^2 \quad (1.4)$$

and $\mathcal{N} = \sqrt{4|k^0 k'^0|}$ is the relativistic normalization factor. The basis of tensor structures is chosen to isolate first the classical term

$$\langle 0 | T_{\mu\nu}(0) | k' k \rangle \Big|^\text{tree} \mathcal{N} = \left(k_{[\mu} \epsilon_{\alpha]} k'_{[\nu} \epsilon'_{\beta]} + k_{[\nu} \epsilon_{\alpha]} k'_{[\mu} \epsilon'_{\beta]} \right) \eta^{\alpha\beta} - \frac{1}{2} \eta_{\mu\nu} k^{[\alpha} \epsilon^{\beta]} k'_{[\alpha} \epsilon'_{\beta]} \quad (1.5)$$

associated to the free-photon $T_{\mu\nu}^{(\gamma)}$ in Eq. (B.1), then the identically conserved terms $P_{\mu\nu}(q)$ associated to the so-called improvement terms, and finally the projector $p_\mu p_\nu$ which is orthogonal to q_μ , and hence conserved, via the on-shell condition. Their physical meaning is made manifest by the dependence on the helicities h and h'

$$\langle 0 | T^{\mu\nu}(0) | k'^{h'} k^h \rangle \mathcal{N} = \begin{pmatrix} \frac{1}{2} \langle k' \sigma^\mu k \rangle \langle k' \sigma^\nu k \rangle F_1(t) & -\langle k k' \rangle^2 (P^{\mu\nu}(q) F_2(t) + p^\mu p^\nu F_3(t)) \\ -[k k']^2 (P^{\mu\nu}(q) F_2(t) + p^\mu p^\nu F_3(t)) & \frac{1}{2} \langle k \sigma^\mu k' \rangle \langle k \sigma^\nu k' \rangle F_1(t) \end{pmatrix} \quad (1.6)$$

where the diagonal entries correspond to $h' = -h = \pm$ (here referred to as helicity-preserving, in reference to the crossed process), while the off-diagonal entries correspond to $h = h' = \pm$ (helicity-flipping). Here, σ^ν are the Pauli matrices, and the square and angle brackets are the standard spinor helicity variables (see App. A). One can recognize the three covariant little-group structures: F_1 parametrizes the helicity-preserving scattering against an off-shell graviton (equivalently on-shell massive spin-2), while F_2 and F_3 control two different helicity-flipping photon scatterings. From the normalization $\lim_{k' \rightarrow k} \langle k'^h | T^{\mu\nu}(0) | k^h \rangle = k^\mu k^\nu / k^0$ associated to the particle 4-momentum $P^\mu |k\rangle = \int d^3x T^{0\mu}(x) |k\rangle = k^\mu |k\rangle$, the helicity-preserving entries of Eq. (1.6) are fixed at zero-momentum transfer

$$F_1(t \rightarrow 0) = 1. \quad (1.7)$$

Once coupled to gravity, this corresponds to the universal helicity-preserving low-energy coupling of gravity set by the reduced Planck mass $m_{\text{Pl}} = (8\pi G)^{-1/2}$, where G is the Newton constant.

1.1 Self-Stress at One Loop

The energy-momentum tensor we consider is defined operationally as the covariant source of a weak gravitational field. At tree-level $F_1 = 1$ and $F_{2,3} = 0$ for all values of t , corresponding to matrix elements of the various free $T_{\mu\nu}$ reported in App. B. At one-loop, radiative corrections modify these values via loops of charged states coupled to the photons,³ and in the following we reconstruct the radiative self-stress matrix elements from tree-level amplitudes using on-shell methods.

³There are in general also loop corrections to F_2 from the vacuum expectation value (VEV) of *neutral* scalars non-minimally coupled to gravity, $\propto \xi \int \sqrt{-g} R H^2 + \dots$, so that a non-vanishing $\langle H \rangle = v$ generates graviton/scalar mixing $\propto v\xi$. See Section 1.2 and Appendix C.

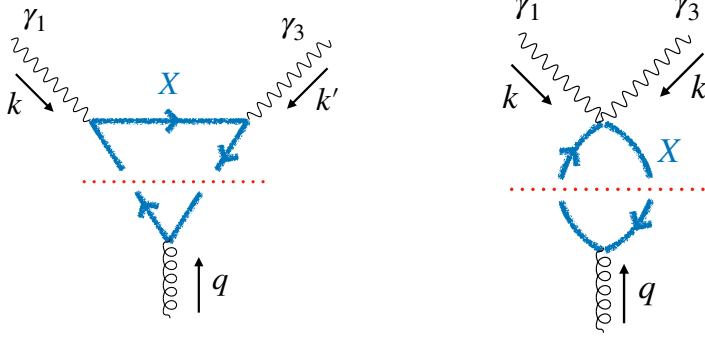


Figure 2: Diagrams contributing to the one-loop discontinuity of the 3pt function (1-3 crossed triangle diagrams omitted for simplicity). Curly lines are graviton legs, wiggly lines represent photons, charged particles in the loop are represented by $X = \phi, \psi, W$, and dotted lines put legs that they cut on-shell.

One simple and efficient way to extract the form factors F_i is calculating first their discontinuities in the complex t -plane across the real line for $t > 4m^2$, as shown in the loop diagrams in Fig. 2, where m is the mass of any given charged state running in the loop. Then one computes the real parts by a simple dispersive integral, see Eq. (1.11). It turns out, in fact, that the gravitational phase shift and the associated light-bending and time delays can be extracted directly from the discontinuity alone (see for example Eqs. (2.6), (2.7) combined with (2.9)).

The discontinuity at one loop can be calculated by either explicit evaluation of the (non-analytic part of the) triangle and bubble diagrams in Fig. 2 (with no cuts), or equivalently by convoluting tree-level amplitudes via the Cutkosky rule. We follow the latter approach and have found it convenient to build first an auxiliary 2-to-2 scattering amplitude $1_\gamma 3_\gamma \rightarrow 2_S 4_S$ for photons into some spectators S taken to be a real massless scalar minimally coupled to gravity. The discontinuity of the energy-momentum tensor in the Mandelstam variable $s_{13} \equiv (k_1 + k_3)^2 = t$ for $s_{13} > 4m^2$ is promptly obtained from the auxiliary amplitude multiplied by $s_{13} m_{\text{Pl}}^2$

$$k_2^{(\mu} k_4^{\nu)} \text{Disc} \langle 0 | T_{\mu\nu}(0) | k_1^{h_1} k_3^{h_3} \rangle = m_{\text{Pl}}^2 \text{Disc} s_{13} \mathcal{M}(1_\gamma 3_\gamma \rightarrow 2_S 4_S) \quad (1.8)$$

by factoring out $k_2^{(\nu} k_4^{\mu)}$. This is effectively the same as considering the s_{13} -channel discontinuity of 2-to-1 amplitudes associated to pairs of photons producing an off-shell graviton. The right-hand side of Eq. (1.8) can be calculated at one loop via the Cutkoski rule

$$\text{Disc} \mathcal{M}(1_\gamma 3_\gamma \rightarrow 2_S 4_S) = i \int d\Pi_{56} \mathcal{M}(1_\gamma 3_\gamma \rightarrow 5_X 6_{\bar{X}}) \mathcal{M}(5_X 6_{\bar{X}} \rightarrow 2_S 4_S) \quad (1.9)$$

using the tree-level amplitudes $\mathcal{M}(1_\gamma 3_\gamma \rightarrow 5_X 6_{\bar{X}})$ and $\mathcal{M}(5_X 6_{\bar{X}} \rightarrow 2_S 4_S)$ where $(5_X, 6_{\bar{X}})$ is any pair of charged particles/antiparticles of spin $J_X = 0, 1/2$ or 1 in the Standard Model (hereafter dubbed ϕ, ψ and W respectively), $d\Pi_{56}$ is their Lorentz invariant two-body phase space, and the sum over the helicities of internal particles is left understood. All the relevant amplitudes are summarized in Tab. 1, and the diagrams contributing to the discontinuity are shown in Fig. 2.

For $X = \phi, \psi$, the 4-point functions $\mathcal{M}(1_\gamma 3_\gamma \rightarrow 5_X 6_{\bar{X}})$ are the pair production amplitudes in standard (scalar and spinorial) QED. They can either be obtained by Feynman diagrams from the Lagrangians given in App. E, or recovered from standard on-shell techniques. With the latter approach, unitarity dictates the factorization of the 4-point amplitude into 3-point amplitudes which are completely fixed by little group scaling and dimensional analysis, (for reviews see e.g. [4, 5]).

The case of the massive vector $X = W$ is slightly more delicate because the high energy limits involve extra 3-point vertices relative to the one of massless Yang-Mills, reflecting the presence of the

$\mathcal{M}(1_\gamma^- 3_\gamma^+ \rightarrow 5_X 6_{\bar{X}})$	$\mathcal{M}(1_\gamma^- 3_\gamma^- \rightarrow 5_X 6_{\bar{X}})$	$\mathcal{M}(5_X 6_{\bar{X}} \rightarrow 2_S 4_S)$
$\frac{g^2 \langle 1(k_5 - k_6) 3 \rangle^2}{2(s_{15} - m^2)(s_{16} - m^2)}$	$\frac{2g^2 m^2 \langle 13 \rangle^2}{(s_{15} - m^2)(s_{16} - m^2)}$	$\frac{(s_{25} - m^2)(s_{45} - m^2)}{m_{\text{Pl}}^2 s_{24}} - \xi_\phi \frac{s_{24}}{6m_{\text{Pl}}^2}$
$\frac{g^2 \langle 1(k_6 - k_5) 2 \rangle}{(s_{15} - m^2)(s_{16} - m^2)} (\langle 15 \rangle [36] + \langle 16 \rangle [35])$	$\frac{2g^2 m \langle 13 \rangle^2 \langle 65 \rangle}{(s_{15} - m^2)(s_{16} - m^2)}$	$\frac{s_{25} - s_{45}}{4m_{\text{Pl}}^2 s_{24}} (\langle 6(k_2 - k_4) 5 \rangle + \langle 5(k_2 - k_4) 6 \rangle)$
$\frac{2g^2}{(s_{15} - m^2)(s_{16} - m^2)} (\langle 15 \rangle [36] + \langle 16 \rangle [35])^2$	$\frac{2g^2 \langle 13 \rangle^2 \langle 65 \rangle^2}{(s_{15} - m^2)(s_{16} - m^2)}$	$\frac{-1}{4m_{\text{Pl}}^2 s_{24}} (\langle 6(k_2 - k_4) 5 \rangle + \langle 5(k_2 - k_4) 6 \rangle)^2$

Table 1: Amplitudes relevant in the determination of $\text{Disc } F_i$, where g is the gauge coupling. Each row corresponds respectively to $X = \phi, \psi, W$. Other photon helicities are recovered by replacing holomorphic with anti-holomorphic configurations (and vice-versa). The contact term proportional to ξ_ϕ in the first line is the amplitude counterpart of the scalar non-minimal coupling to gravity, see Eq. 1.15. Other model dependent contributions, such as those due to Higgs bosons, are discussed in Section 1.2. See App. A for conventions.

X	$\text{Disc } F_1(t \gg m^2)$	$\text{Disc } F_2(t \gg m^2)$	$\text{Disc } F_3(t \gg m^2)$
ϕ	$\frac{i\alpha}{6}$	$\frac{i\alpha}{12}(5 - 4\xi_\phi)\delta(t)$	$-\frac{i\alpha}{12}\delta(t)$
ψ	$\frac{2i\alpha}{3}$	$\frac{i\alpha}{6}\delta(t)$	$\frac{i\alpha}{6}\delta(t)$
W	$-\frac{i\alpha}{2}(7 - 4 \log \frac{t}{m^2})$	$-\frac{i3\alpha}{4}\delta(t)$	$-\frac{i\alpha}{4}\delta(t)$

Table 2: Large t limit of $\text{Disc } F_i$.

eaten Goldstone bosons. The minimal cubic coupling we consider is thus fixed by its high energy behavior, requiring that the vertices match massless Yang-Mills for the transverse polarizations, and minimally coupled massless scalars for the longitudinal polarizations. This is simply the on-shell amplitude description of the Higgs mechanism [6], i.e. the Goldstone equivalence theorem. Once again, this result is matched by the Lagrangian formulation of App. E. The last column of Tab. 1 is the production of the neutral spectator through the gravitational interaction. All X are taken to couple minimally to gravity except for the non-minimal coupling present on Tab. 1 for ϕ , parametrized by ξ_ϕ . Such a contribution is discussed in Section 1.2.

Comparing the tensor structures in Eq. (1.3) or Eq. (1.6) with the expressions we find for Eq. (1.8) using Eq. (1.9) and the amplitudes in Tab. 1, we extract the form factor discontinuities $\text{Disc } F_i$. For convenience, we list here $\text{Disc } F_1$ for the three massive spinning particles ϕ, ψ, W running in the loop, while the discontinuities of the other form factors are reported in App. D

$$\begin{aligned}
\text{Disc } F_1(t)_\phi &= \frac{i\alpha}{6t^2} \left(t(t - 10m^2) \sqrt{1 - \frac{4m^2}{t}} + 24m^4 \tanh^{-1} \sqrt{1 - \frac{4m^2}{t}} \right) \theta(t - 4m^2) \\
\text{Disc } F_1(t)_\psi &= \frac{2i\alpha}{3t^2} \left(\sqrt{1 - \frac{4m^2}{t}} (5m^2 + t) t - 6m^2 (2m^2 + t) \tanh^{-1} \sqrt{1 - \frac{4m^2}{t}} \right) \theta(t - 4m^2) \\
\text{Disc } F_1(t)_W &= \frac{-i\alpha}{2t^2} \left(\sqrt{1 - \frac{4m^2}{t}} t (10m^2 + 7t) - 8(m^2 + t)(3m^2 + t) \tanh^{-1} \sqrt{1 - \frac{4m^2}{t}} \right) \theta(t - 4m^2).
\end{aligned} \tag{1.10}$$

where $\theta(x)$ is the Heaviside uni-step function and $\alpha = g^2/4\pi$ is the fine structure constant. The $t \gg m^2$ limits of these expressions will be very useful in the following discussion and therefore are listed in Tab. 2.

While $\text{Disc } F_{2,3}(t/m^2 \rightarrow \infty)$ vanish pointwise, they actually return Dirac δ -functions since they

X	$F_1(t)$		$F_2(t)$		$F_3(t)$	
	$m^2 \gg t$	$m^2 \ll t$	$m^2 \gg t$	$m^2 \ll t$	$m^2 \gg t$	$m^2 \ll t$
ϕ	$1 + \frac{\alpha t}{180\pi m^2}$	$1 + \frac{\alpha}{72\pi} (19 - 6 \log \frac{-t}{m^2})$	$\frac{\alpha(13-10\xi_\phi)}{720\pi m^2}$	$-\frac{\alpha(5-4\xi_\phi)}{24\pi t}$	$-\frac{\alpha}{720\pi m^2}$	$\frac{\alpha}{24\pi t}$
ψ	$1 + \frac{11\alpha t}{360\pi m^2}$	$1 + \frac{\alpha}{\pi} (\frac{35}{36} - \frac{1}{3} \log \frac{-t}{m^2})$	$\frac{\alpha}{180\pi m^2}$	$-\frac{\alpha}{12\pi t}$	$\frac{\alpha}{360\pi m^2}$	$-\frac{\alpha}{12\pi t}$
W	$1 + \frac{7\alpha t}{20\pi m^2}$	$1 - \frac{\alpha}{4\pi} (\frac{125}{6} - 7 \log \frac{-t}{m^2} + 2 \log^2 \frac{-t}{m^2})$	$-\frac{7\alpha}{240\pi m^2}$	$\frac{3\alpha}{8\pi t}$	$-\frac{\alpha}{240\pi m^2}$	$\frac{\alpha}{8\pi t}$

Table 3: Large m limit of the form factors F_i .

X	α_1	α_2	α_3
ϕ	$\frac{\alpha}{288\pi m^2} (1 - \xi_\phi)$	$\frac{\alpha}{360\pi m^2}$	$\frac{\alpha}{720\pi m^2}$
ψ	$-\frac{\alpha}{144\pi m^2}$	$\frac{13\alpha}{360\pi m^2}$	$-\frac{\alpha}{360\pi m^2}$
W	$-\frac{3\alpha}{32\pi m^2}$	$\frac{41\alpha}{240\pi m^2}$	$\frac{\alpha}{240\pi m^2}$

Table 4: Low energy matching of the form factors to the effective couplings of Eq. (1.12)

return $f(0)$ when properly normalized and integrated against a test function $f(t)$ in the limit $t/m^2 \rightarrow \infty$. Notice that the constant contribution to $\text{Disc } F_1(t \gg m^2)$ is given by the β -function of the corresponding particle in the loop, as detailed in Sec. 1.3. Also, the behavior of the massive spin-1 particle differs from the other contributions by the presence of a $\log t/m^2$ which will be identified as the contribution of soft divergences.

The discontinuities can thus be integrated with the dispersion relations

$$F_1(t) = 1 + \frac{t}{2\pi i} \int_{4m^2}^{\infty} \frac{dt'}{t'} \frac{\text{Disc } F_1(t')}{t' - t - i0^+}, \quad F_{2,3}(t) = \frac{1}{2\pi i} \int_{4m^2}^{\infty} dt' \frac{\text{Disc } F_{2,3}(t')}{t' - t - i0^+}. \quad (1.11)$$

determining F_i everywhere in the complex cut t -plane. The subtraction constant for F_1 has been fixed by the normalization condition (1.7), so that helicity-preserving low-energy photons scatter gravitationally with strength $1/m_{\text{Pl}}$. The full expressions of $F_i(t)$ are summarized in App. D, while the important limits are collected in Tab. 3 for convenience. The earliest calculation of F_i in spinorial QED was performed in [7].

One particularly interesting limit of Eq. (1.3) is at large masses of the particles running in the loop. This limit is equivalent to integrating out such particles and can be matched to effective irrelevant contributions displayed by the $\alpha_{i=1,2,3}$ Wilson coefficients in the following effective Lagrangian⁴

$$\mathcal{L} = -\frac{1}{4} F_{\mu\nu} F^{\mu\nu} + \alpha_1 R F_{\mu\nu} F^{\mu\nu} + \alpha_2 R_{\mu\nu} F^{\mu\alpha} F_{\alpha}^{\nu} + \alpha_3 R_{\mu\nu\alpha\beta} F^{\mu\nu} F^{\alpha\beta} + \dots \quad (1.12)$$

By computing how the coefficients α_i enter in the matrix element of the energy-momentum tensor, we can match their contribution to the large m limit of the form factors. The explicit values of the effective couplings α_i we calculated are given in Tab. 4.

Notice that the form factor F_3 reduces to the Wilson coefficient of $F_{\mu\nu} F_{\alpha\beta} R^{\mu\nu\alpha\beta}$ i.e. $\alpha_3 = -F_3(t \ll m^2)$, which give rise to on-shell helicity-violating 3-point vertex $\gamma\gamma$ – graviton, at low energy. The $\alpha_{1,2}$

⁴Wilson coefficients of four field-strength operators like $(F_{\mu\nu} F^{\mu\nu})^2$ are also present but would contribute to the form factors in Eq. (1.3) only at higher order.

correct instead low-energy 4-point amplitudes only, as is visible by using the equations of motion. The electron and scalar Wilson coefficients for α_3 nicely agree with the results present in the literature, see e.g. [3, 7, 8] and references therein. The effective Wilson contribution from massive vectors is new to the best of our knowledge.

1.2 Non-Minimal Couplings and Higgs/Graviton Mixing

The (ξ_ϕ -independent part of the) form factors we have calculated are generated at one loop by charged states minimally coupled to photons and gravity. Within this setup neutral particles contribute from 2-loop order only. With non-minimal couplings, instead, other 1-loop contribution are generated, even from neutral scalars.

In this subsection we discuss two illustrative cases of non-minimal gravitational coupling for charged (ϕ) and neutral (H) scalars. The latter is actually relevant because of the Higgs mechanism whenever charged spin-1 particles are considered, should the Higgs boson be coupled to gravity non-minimally. We report the result for the Standard Model Higgs at the end of this subsection.

Let us consider non-minimal gravitational couplings given by

$$S \supset \int d^4x \frac{R}{6} \left(\xi_\phi |\phi|^2 + \frac{\xi_H}{2} H^2 \right) \implies \delta T_{\mu\nu} = -\frac{1}{3} (\partial_\mu \partial_\nu - \eta_{\mu\nu} \square) \left(\xi_\phi |\phi|^2 + \frac{\xi_H}{2} H^2 \right), \quad (1.13)$$

where we extracted the energy-momentum tensor from the linear gravitational coupling around Minkowski, that is $\delta S = \int d^4x \sqrt{-g} T_{\mu\nu} \delta g^{\mu\nu} / 2$. They clearly contribute to identically conserved improvement terms of the energy-momentum tensor, hence changing the F_2 form factor in Eq. (1.3). The case with $\xi_\phi = \xi_H = 1$ and vanishing masses is known as conformally coupled scalars because the two-derivative action becomes classically Weyl invariant.

One simple way to take the effect of $\xi_{\phi,H}$ into account, which makes also direct contact with the on-shell method approach we have taken in the rest of this work, is by removing the non-minimal couplings via a field redefinition that is effectively equivalent to plugging the unperturbed equation of motion $R = -T_\mu^\mu / m_{\text{Pl}}^2$ in the action in Eq. (1.13).⁵ This gives rise to new contact-term interactions associated to the trace of energy-momentum tensor

$$S \supset \int d^4x \frac{1}{6m_{\text{Pl}}^2} \left(\xi_\phi |\phi|^2 + \frac{\xi_H}{2} H^2 \right) [(\partial S)^2 + 2|\partial\phi|^2 + (\partial H)^2 + \dots]. \quad (1.14)$$

Therefore, the effect of non-minimal coupling associated to ξ_ϕ is nothing but changing the on-shell data that enter in the calculation of the discontinuities, i.e.

$$\delta \mathcal{M}(5_\phi 6_{\bar{\phi}} \rightarrow 2_S 4_S) = -\frac{\xi_\phi}{6} \frac{s_{24}}{m_{\text{Pl}}^2}, \quad (1.15)$$

as reported in the first row of Tab. 1, the first row of Tab. 3, and more generally in the F_2 reported in App. D.

On the other hand, ξ_H does not affect F_2 at one loop (to $O(1/m_{\text{Pl}}^2)$) unless H gets a VEV $\langle H \rangle = v$ and it couples to charged states running in the loop, both conditions being actually satisfied for the neutral component for the Higgs boson field of the Standard Model. Indeed, from the $\delta T_{\mu\nu}$ in Eq. (1.13), after replacing the perturbations around the VEV, we have

$$\langle 0 | \delta T_{\mu\nu}^{(H)}(0) | \gamma\gamma \rangle = \frac{\xi_H v}{3} (q_\mu q_\nu - \eta_{\mu\nu} q^2) \frac{-1}{s_{13} - m_H^2} \mathcal{M}(1_\gamma 3_\gamma \rightarrow H) \quad (1.16)$$

⁵See Appendix C for an equivalent discussion phrased in terms of Higgs/graviton mixing resolved by field redefinitions.

where m_H is the Higgs boson mass, and the amplitude $\mathcal{M}(1_\gamma 3_\gamma \rightarrow H)$ is model dependent. The latter depends on the trilinear Higgs boson coupling $HX\bar{X}$ where X is running in the loop. Eq. (1.16) produces as well a shift in the on-shell scattering data between the Higgs and the spectator field

$$\delta\mathcal{M}(1_\gamma 3_\gamma \rightarrow 2_S 4_S) = \mathcal{M}(1_\gamma 3_\gamma \rightarrow H) \left(\frac{s_{13}}{s_{13} - m_H^2} \right) \left(\frac{v\xi_H}{6m_{\text{Pl}}^2} \right) \quad (1.17)$$

as one can also check directly from Eq. (1.14).

Let's put these expressions to good use and consider the example of $SU(2) \rightarrow U(1)$ symmetry breaking pattern for a weakly coupled $SU(2)$ gauge theory where a real triplet $\vec{\phi}$ gets the VEV $\langle\phi^i\rangle = \delta^{i3}v$. The low-energy physical spectrum contains a massless photon and, since the theory is weakly coupled, it contains as well a pair of spin-1 bosons W^\pm of mass $m_W^2 = (gv)^2$ and a neutral Higgs boson H in $\vec{\phi} = (\pi^1, \pi^2, v + H)$. For convenience, we now call H the fluctuation around the VEV. Everything we discussed in this subsection applies directly to ϕ_3 in the unitary gauge where $\int d^4x \xi_H R \vec{\phi}^2/12 = \int d^4x \xi_H R(v + H)^2/12$. The amplitude in the $s_{13} \gg m_W^2$ and $s_{13} \ll m_W^2$ limits is extracted immediately via the Goldstone equivalence theorem (see e.g. [9,10]) and the Higgs low-energy theorem [11], respectively,

$$\begin{aligned} \frac{\mathcal{M}(1_\gamma 3_\gamma \rightarrow H)}{[2(\epsilon' \cdot k)(\epsilon \cdot k') - q^2(\epsilon \cdot \epsilon')]} \Big|_{s_{13} \gg m_W^2} &= -\frac{2}{v} \left(\frac{\alpha}{4\pi} \right), \\ \frac{\mathcal{M}(1_\gamma 3_\gamma \rightarrow H)}{[2(\epsilon' \cdot k)(\epsilon \cdot k') - q^2(\epsilon \cdot \epsilon')]} \Big|_{s_{13} \ll m_W^2} &= -\frac{7}{v} \left(\frac{\alpha}{4\pi v} \right) \end{aligned} \quad (1.18)$$

so that Eq. (1.16) compared to Eq. (1.3) returns

$$\delta F_2(t) \Big|_{t \gg m_W^2} = \frac{2\xi_H}{3} \left(\frac{\alpha}{4\pi} \right) \frac{1}{t - m_H^2}, \quad \delta F_2(t) \Big|_{t \ll m_W^2} = \frac{7\xi_H}{3} \left(\frac{\alpha}{4\pi} \right) \frac{1}{t - m_H^2}, \quad (1.19)$$

where we remind the reader that $s_{13} = t$. The $t \gg m_{H,W}^2$ limit of $t \delta F_2(t)$ in Eq. (1.19) enters directly in the trace anomaly equation we will discuss in Sec. 1.3.

Next we move to the result for δF_2 valid for all s_{13} . Since this model contains the same spectrum and couplings of the particles that generate the spin-1 contribution to the $H \rightarrow \gamma\gamma$ process in the Standard Model, we can directly use the W -boson contribution from the Standard Model expression of $\mathcal{M}(1_\gamma 3_\gamma \rightarrow H)$ which, incidentally can also be extracted by dispersion relations and on-shell data [12] being careful with the subtraction constants that can be fixed by matching to the Goldstone equivalence theorem and the Higgs low-energy theorem results. From the Standard Model W -contribution to $\mathcal{M}(1_\gamma 3_\gamma \rightarrow H)$ we thus get

$$\delta F_2(t) = \frac{2\xi_H}{3} \frac{\left(\frac{\alpha}{4\pi}\right)}{t - m_H^2} \left\{ 1 + 6 \frac{m_W^2}{t} - 3 \frac{m_W^2}{t} \left(1 - 2 \frac{m_W^2}{t} \right) \left(\log \frac{1 + \sqrt{1 - 4m_W^2/t}}{1 - \sqrt{1 - 4m_W^2/t}} - i\pi \right)^2 \right\}. \quad (1.20)$$

A similar contribution from the top-quark can easily be included as well in $\mathcal{M}(1_\gamma 3_\gamma \rightarrow H)$, so that Eq. (1.16) can be used to determine δF_2 contribution from the Higgs boson of the Standard Model.

1.3 Trace Anomaly and the Running Coupling

The trace of the energy-momentum tensor is

$$\begin{aligned} \langle 0 | T_\mu^\mu(0) | k'^h k^h \rangle &= -t (3F_2(t) + F_3(t)) [2(\epsilon' \cdot k)(\epsilon \cdot k') - q^2(\epsilon \cdot \epsilon')] \\ &= t (3F_2(t) + F_3(t)) \begin{pmatrix} 0 & \langle kk' \rangle^2 \\ [kk']^2 & 0 \end{pmatrix}, \end{aligned} \quad (1.21)$$

which depends only on the combination $t(3F_2 + F_3)$ and is non-zero only for helicity-flipping photons, as it should be for the overlap of photons with the spin-0 state $\langle 0|T_\mu^\mu(0)$.

For $t \gg 4m^2$ and $t \gg m_H^2$, i.e. well above the pair production threshold of massive charged particles and Higgs bosons, and setting $\xi_\phi = \xi_H = 1$ for all conformal couplings in (1.14), the QED trace anomaly

$$T_\mu^\mu = \frac{\beta}{2g} F_{\rho\sigma}^2, \quad (1.22)$$

implies $\langle 0|T_\mu^\mu|k'k\rangle\mathcal{N} = \frac{\beta}{g} [2(\epsilon' \cdot k)(\epsilon \cdot k') - q^2(\epsilon \cdot \epsilon')]$. Therefore Eq. (1.21) allows us to express the β -function for the gauge coupling $g = g(\mu)$ in terms of the form factors

$$\beta = -g \lim_{t/m^2 \rightarrow \infty} t [3F_2(t) + F_3(t)]_{\xi_{\phi,H}=1}. \quad (1.23)$$

From the explicit expressions that we calculated, see Tab. 3 and Eq. (1.19), we can read off the QED β -functions from loops of charged spin-0, spin-1/2 and spin-1 particles (for unit charges) as

$$\beta_\phi = \frac{1}{3} \left(\frac{g^3}{16\pi^2} \right), \quad \beta_\psi = \frac{4}{3} \left(\frac{g^3}{16\pi^2} \right), \quad \beta_W = -7 \left(\frac{g^3}{16\pi^2} \right) \quad (1.24)$$

In β_W we included the contribution from the Higgs/graviton mixing, Eq. (1.19).

It is a highly non-trivial result that from gravitational form factors we correctly reproduce the non-abelian (negative) $SU(2)$ β -function $\beta_W/(g^3/16\pi^2) = -11/3 \times 2 + 1/6 \times 2 = -7$, including the scalar matter in the adjoint representation, and using purely on-shell data associated to scattering only physical polarizations. This connection between the energy-momentum tensor, scattering data, and the β -functions is somewhat reminiscent of the methods presented in [13].

We remark that the finite value at $t/m^2 \rightarrow \infty$ of the β -functions as calculated by the trace anomaly boils down to the presence of an IR-localized Dirac δ -function in $\text{Disc } F_{2,3}$ that we have reported in Tab. 2. These Dirac δ -functions represent the IR side of the trace anomaly in full analogy with the chiral anomaly case, see [14, 15], as it was already pointed out for spinorial QED in [16]. By contrast, we explore below the UV side associated to the running coupling and expose its connection to the F_1 form factor.

By putting the theory on a curved spacetime⁶

$$S = \int d^4x \sqrt{|g|} \left\{ -\frac{1}{4g^2(\mu)} F_{\mu\nu} F^{\mu\nu} - \frac{m_{\text{Pl}}^2}{2} R + \dots \right\} \quad (1.25)$$

we can as well establish an important connection between the β -function and the F_1 form factor which is directly connected to the asymptotic time delay at short impact parameter, as we show in Sec. 2. Expanding the action (1.25) to first order in the metric perturbations around Minkowski spacetime and Fourier-transforming the photon field (with a slight abuse of notation) $\epsilon_\mu(k) = \int d^4x e^{ikx} A_\mu(x)$ we get

$$S \supset - \int \frac{d^4q}{(2\pi)^4} \frac{d^4k'}{(2\pi)^4} \frac{d^4k}{(2\pi)^4} (2\pi)^4 \delta^4(q+k+k') h^{\mu\nu}(q) \frac{1}{2g^2(\mu)} \langle 0|T_{\mu\nu}(0)|k'k\rangle^{\text{tree}} \mathcal{N} + \dots \quad (1.26)$$

The same running coupling $g = g(\mu)$ in front of the photon kinetic term is found as well in the F_1 form factor. That is, the counter-term needed to renormalize the photon kinetic term also enters in the F_1 form factor. Therefore, in the limit $q^2 \gg m^2$, rather than defining $g(\mu)$ as the coupling of an off-shell

⁶The gauge coupling $g = g(\mu)$ should not be confused with the metric determinant in the volume element $\sqrt{|g|}d^4x$.

A_μ to charged currents, as e.g. measured in the Coulomb potential at a floating renormalization scale $-q^2 = \mu^2$ (i.e. in a scattering process mediated by a virtual photon), we can equally think of it as the coupling of two incoming helicity-preserving on-shell photons scattering on an off-shell graviton with $-t = \mu^2$

$$\frac{d}{d \log \mu} \frac{1}{g^2(\mu)} = \frac{d}{d \log \mu} F_1(t = -\mu^2)|_{m \ll \mu, g=1} \implies \beta = -\frac{g}{2} \frac{d}{d \log \mu} F_1(t = -\mu^2)|_{m \ll \mu}. \quad (1.27)$$

In the right-most expression in Eq. (1.27) we have restored to a canonically normalized kinetic term $-1/4 F_{\mu\nu}^2$ in the lagrangian density. The formula in (1.27) links directly the sign of the $\log(-t)$ in the helicity-preserving form factor F_1 to the sign of the β -function.⁷ Moreover, from the dispersion relations Eq. (1.11) the $\log(-t)$ arises, in the case of spinorial and scalar QED, by the constant limit of the discontinuity $\text{Disc } F_1(t \rightarrow \infty)$, hence

$$\beta_{\phi, \psi} = \lim_{t/m^2 \rightarrow \infty} \frac{g}{\pi} \frac{\text{Disc } F_1(t)}{2i}. \quad (1.28)$$

This nice expression connects directly the β -function in spinorial and scalar QED to the discontinuity of the helicity-preserving gravitational form factor F_1 , i.e. to on-shell-only gravitational scattering amplitudes. From the first two rows of the first column of Tab. 2 one indeed reproduces the β_ϕ and β_ψ in Eq. 1.24.

1.4 IR-Divergences and Sudakov Double-Logarithms

The presence of a finite —but still large— \log^2 factor in the high energy limit of the helicity-preserving form factor F_1 generated at one loop by massive charged spin-1 W bosons

$$\frac{\langle 0 | T_{\mu\nu}(0) | 1_\gamma^- 3_\gamma^+ \rangle^{(1\text{-loop})}}{\langle 0 | T_{\mu\nu}(0) | 1_\gamma^- 3_\gamma^+ \rangle^{\text{tree}}} \xrightarrow{t/m_W^2 \rightarrow \infty} 1 - \frac{\alpha}{4\pi} \left(\frac{125}{6} - 7 \log \frac{-t}{m_W^2} + 2 \log^2 \frac{-t}{m_W^2} \right) \quad (1.29)$$

can be understood as the IR divergences that we would encounter if the W mass were vanishing. It arises in a way that is completely analogous to the presence of large double-logarithms in the matrix elements of electroweak currents, see e.g. [17–19], which are usually called electroweak Sudakov double-logarithms in analogy to the original QED Sudakov factors that are associated to the vanishing photon mass.

In the present context we deal with these gravitational Sudakov factors by taking a renormalization group approach to resum the leading double-log factors. We first regulate the most IR-singular class of diagrams by cutting them with a floating mass $m_W \rightarrow m = \mu$, which should be taken not too far from the kinematical variables so that perturbation theory is reliable, and then we evolve the form factor down with the resulting RG equation that we can thus write as an evolution in the mass, namely

$$\frac{\partial \langle 0 | T_{\mu\nu}(0) | 1_\gamma^- 3_\gamma^+ \rangle}{\partial \log(m^2/(-t))} = -4 \left(\frac{\alpha}{4\pi} \right) \log \left(\frac{-t}{m^2} \right) \langle 0 | T_{\mu\nu}(0) | 1_\gamma^- 3_\gamma^+ \rangle. \quad (1.30)$$

Integrating this RG equation from $\mu = \mu_0$ down to the W mass $\mu = m_W$ we get the exponentiation of the Sudakov double-logs in the form factor

$$F_1(t) \simeq F_1(\mu_0^2) \text{Exp} \left[-2 \left(\frac{\alpha}{4\pi} \right) \left(\log^2 \frac{m_W^2}{-t} - \log^2 \frac{\mu_0^2}{-t} \right) \right] \quad (1.31)$$

⁷Trading the $\log \mu^2$ dependence for the $\log q^2$ breaks down, however, if extra $\log q^2/m^2$ factors survive in the $q^2 \gg m^2$ limit, which signals the presence of IR divergences. They do not arise at one loop of spin-0 and spin-1/2 charged states, but are instead present for spin-1 particles for which, therefore, Eq. (1.27) and (1.28) no longer apply. We study IR divergences in Sec. 1.4.

and the associated exponential suppression for $t \gg m_W^2$

$$|F_1(t \gg m_W^2)| \propto (|t|/m_W^2)^{-2(\alpha/4\pi) \log |t|/m_W^2} \rightarrow 0 \quad (1.32)$$

at high-energy. The imaginary part of F_1 has an oscillatory $\sin(\alpha \log |t|/m_W^2)$ factor but in fact does not change sign within the range of validity of perturbation theory.

While the exponential suppression we find is analogous to the vanishing of exclusive processes in ordinary QED, here the W mass is finite and this makes the resummed form factor and the associated exclusive amplitudes actually finite. Moreover, the finiteness of the W mass and charge allow one to distinguish states with different numbers of W particles in them, contrary to the case of the photon emissions which can always escape detections if sufficiently soft. For these reason we keep working in the following with the exclusive matrix elements rather than inclusive cross-sections for what concerns additional W emissions.

2 The Phase Shift

Now that the form factors $F_i(t)$ have been determined, we proceed to computing various quantities of interest. We study the 4-point function (diagrammatically shown in Fig. 1) in the eikonal limit $s \gg t$, where the center of mass energy is much larger than the exchanged momentum. In this limit, the amplitude is dominated by ladder and crossed ladder diagrams, which can be written as a geometric series of convolutions. The amplitude exponentiates in impact parameter space as $e^{2i\delta(s,b)}$, where $\delta(s,b)$, referred to as the phase shift, is related to a number of observables such as the time delay, as explicitly shown in Sec. 3.1. A large phase in the eikonal limit is generated perturbatively when considering a coherent state of spectators as explained in [2] as well as in transplanckian scattering [20–22]. The leading quantum corrections in the gauge coupling to the phase shift are presented in this section.

2.1 Amplitudes in the Eikonal Limit

In this section, we present the eikonal limit of the 4-point amplitude, which will be used in the evaluation of the time delay, following [2, 23]. For simplicity, we detail the construction for a scalar spectator, but we have checked that in the eikonal limit, the same result is obtained by scattering against spin-1 and spin-2 spectators minimally coupled to gravity. In other words, the spin of the spectator is irrelevant in the computation of the time delay, as long as it is characterized only by a minimal gravitational interaction.

When contracted with the scalar 3-point function, the full amplitude takes the form

$$\mathcal{M}(1_\gamma 3_\gamma \rightarrow 2_S 4_S) = \begin{pmatrix} -\frac{\langle 3k_2 1 \rangle^2}{m_{\text{Pl}}^2 s_{13}} F_1(t) & \frac{\langle 13 \rangle^2}{2m_{\text{Pl}}^2} \left(s_{13} F_2(t) + \frac{(s_{12}-s_{14})^2}{s_{13}} F_3(t) \right) \\ \frac{\langle 13 \rangle^2}{2m_{\text{Pl}}^2} \left(s_{13} F_2(t) + \frac{(s_{12}-s_{14})^2}{s_{13}} F_3(t) \right) & -\frac{\langle 1k_2 3 \rangle^2}{m_{\text{Pl}}^2 s_{13}} F_1(t) \end{pmatrix} \quad (2.1)$$

where we recall that the diagonal entries correspond to the helicity preserving amplitudes with $h' = -h = \pm$ while the off-diagonal entries correspond to the helicity-flipping $h = h' = \pm$, and the Mandelstam variables s_{ij} are defined in App. A. This amplitude is evaluated on the following massless kinematic configuration

$$\begin{aligned} k_1^\mu &= (\omega, -\vec{p} + \vec{q}/2) , & k_3^\mu &= -(\omega, -\vec{p} - \vec{q}/2) , \\ k_2^\mu &= (\omega, \vec{p} - \vec{q}/2) , & k_4^\mu &= -(\omega, \vec{p} + \vec{q}/2) , \end{aligned} \quad (2.2)$$

where \vec{q} is the exchanged momenta, $\omega = \sqrt{\vec{p}^2 + \vec{q}^2}/4$, and in the following we fix the direction of $\vec{p} = p\hat{z}$, where \hat{z} is the unit vector in the z -direction. The Mandelstam variables in this configuration are given by

$$s = s_{12} = 4\omega^2, \quad t = s_{13} = -\vec{q}^2, \quad u = s_{14} = -4\vec{p}^2 \quad (2.3)$$

By momentum conservation, the product $\vec{p} \cdot \vec{q}$ is zero, implying that the momentum transfer \vec{q} lies in the xy -plane. With an abuse of notation, we will refer to \vec{q} as a two-dimensional vector with components $\vec{q} = (q_1, q_2)$.

We are interested in the eikonal approximation $\omega \gg |\vec{q}|$, where the amplitude Eq. (2.1) in the kinematic configuration Eq. (2.2) is given by

$$\mathcal{M}^{\text{eik}}(t) = \frac{s^2}{m_{\text{Pl}}^2 \vec{q}^2} \begin{pmatrix} F_1(t) & -4q_+^2 F_3(t) \\ -4q_-^2 F_3(t) & F_1(t) \end{pmatrix}, \quad (2.4)$$

where $q_+ = \frac{1}{\sqrt{2}}(q_1 + iq_2)$ and $q_- = \frac{1}{\sqrt{2}}(q_1 - iq_2)$. Notice that in the eikonal regime the form factor $F_2(t)$ is subleading and will not enter in the phase shift. This means that the improvement terms proportional to ξ_ϕ and ξ_H do not produce any measurable effect on the time delay.

2.2 Computation of the Phase Shift

The phase shift is obtained by Fourier transforming the 4-point amplitude in the eikonal limit Eq. (2.4) to impact parameter space

$$\delta(s, b) = \frac{1}{4s} \int \frac{d^2 q}{(2\pi)^2} e^{i\vec{b} \cdot \vec{q}} \mathcal{M}^{\text{eik}}(t = -\vec{q}^2), \quad (2.5)$$

where $b \equiv |\vec{b}|$. The eigenvalues of this matrix are given by

$$\delta_\pm(s, b) = \frac{s}{4m_{\text{Pl}}^2} \left[\hat{F}_1(b^2) \pm 16b^2 \hat{F}_3''(b^2) \right], \quad (2.6)$$

where we have defined

$$\hat{F}_i(b^2) = \int \frac{d^2 q}{(2\pi)^2} \frac{F_i(-\vec{q}^2)}{\vec{q}^2} e^{i\vec{b} \cdot \vec{q}}, \quad (2.7)$$

for $i = 1, 3$, and $\hat{F}_3' \equiv \partial \hat{F}_3 / \partial b^2$.

The integrand in Eq. (2.7) is discontinuous at the graviton pole or above threshold, i.e. when $q_1 = \pm iq_2$ or $t = -\vec{q}^2 > 4m^2$. We can then compute Eq. (2.7) by applying the Cauchy theorem. The integration contour of q_1 can be deformed in its complex plane so to express the integral in terms of the discontinuities computed in Tab. 2, see Fig. 3. Without loss of generality, we can fix $\vec{b} = (b, 0)$ because of rotation invariance. After performing the rotation $q_1 = iQ_1$ and changing the order of integration, Eq. (2.7) takes the form

$$\hat{F}_i(b^2) = -\frac{F_i(0)}{2\pi} \log b/b_{\text{IR}} + \frac{2i}{(2\pi)^2} \int_{2m}^{+\infty} dQ_1 \int_0^{\sqrt{Q_1^2 - 4m^2}} dq_2 \frac{\text{Disc } F_i(Q_1^2 - q_2^2)}{Q_1^2 - q_2^2} e^{-Q_1 b}, \quad (2.8)$$

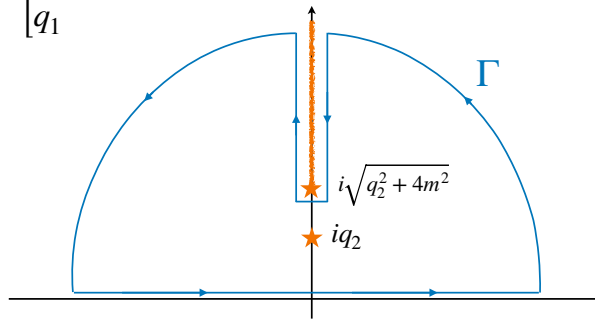


Figure 3: Integral contour Γ in the upper complex q_1 -plane for \hat{F}_i . There are two contributions: one from the graviton pole, and the second from the discontinuity above threshold $t > 4m^2$.

where b_{IR} is an infrared cutoff. The b_{IR} has no physical impact as long as one consider wave-packets with $b < b_{\text{IR}}$. The integral (2.8) can be further simplified by changing variables $Q_1 = \sqrt{t} \cosh \theta$, $q_2 = \sqrt{t} \sinh \theta$, in terms of which it becomes

$$\hat{F}_i(b^2) = -\frac{F_i(0)}{2\pi} \log b/b_{\text{IR}} + \frac{i}{(2\pi)^2} \int_{4m^2}^{+\infty} dt \frac{\text{Disc } F_i(t)}{t} K_0(b\sqrt{t}) , \quad (2.9)$$

where K_0 is the modified Bessel function of the second kind.

Before discussing the whole one-loop calculation, we focus on the tree-level contribution, which corresponds to $F_1(t) = 1$ and $F_2(t) = F_3(t) = 0$. In this case, Eq. (2.6) and Eq. (2.9) return the tree-level contribution to the phase shift as

$$\delta_0(s, b) = -\frac{s}{8\pi m_{\text{Pl}}^2} \log b/b_{\text{IR}} . \quad (2.10)$$

Since the IR cutoff is the largest scale that we consider, Eq. (2.10) always leads to a positive contribution to the phase shift. At one-loop, there are additional contributions coming from $F_i(0)$ and the discontinuity, see Tab. 3. In the following two sections, we study Eq. (2.9) analytically in two opposite regimes in parameter space: $b \gg 1/m$ and $b \ll 1/m$, while the full solution is solved numerically and displayed in Fig. 4.

2.2.1 The Large b Limit

In the scenario $b \gg 1/m$, we can use the asymptotic behavior of the Bessel function $K_0(b\sqrt{t}) \sim e^{-b\sqrt{t}}/\sqrt{bt^{1/2}}$ which shows that the contribution from the integral over the discontinuity is exponentially suppressed. Therefore, the only contribution comes from the graviton pole, and the phase shift is given by

$$\delta_{\pm}(s, b \gg 1/m) = \delta_0(s, b) \pm \frac{sF_3(0)}{\pi m_{\text{Pl}}^2 b^2} , \quad (2.11)$$

where $F_3(0)$ is summarized in Tab. 3 for different spins of the particle in the loop. This is the result one would obtain by working in the EFT where the massive states have been integrated out, and it reproduces the correction from the effective term $F_{\mu\nu}F_{\alpha\beta}R^{\mu\nu\alpha\beta}$ computed first in [2] and discussed at the end of Sec. 1.1. Notice that the only contribution from $F_1(t)$ comes from the tree-level amplitude, as all corrections vanish when evaluated on the pole.

2.2.2 The Small b Limit for Loops of Scalars and Fermions

We can write the integral in Eq. (2.9) in terms of a dimensionless variable $y = b\sqrt{t}$

$$\hat{F}_i(b^2) = -\frac{F_i(0)}{2\pi} \log b/b_{\text{IR}} + \frac{i}{2\pi^2} \int_{2mb}^{+\infty} dy \frac{\text{Disc } F_i(y^2/b^2)}{y} K_0(y) . \quad (2.12)$$

Let us first focus on the helicity preserving contribution $F_1(t)$ to the phase shift in Eq. (2.6). In the small bm regime, the integrand $\text{Disc } F_1(y^2/b^2)$, which is actually a function of the dimensionless ratio y^2/b^2m^2 , receives contribution mostly from the $\text{Disc } F_i(t \rightarrow \infty)$ region, so that we can directly use

$$\text{Disc } F_1(t \gg m^2) \simeq \frac{2i\pi\beta_X}{g} , \quad (2.13)$$

see Eq. (1.28), which nicely links the contribution of the form factors to the time-delay to the β -function. This approximation is valid for scalars $\beta_\phi = \frac{1}{3} \left(\frac{g^3}{16\pi^2} \right)$ and fermions $\beta_\psi = \frac{4}{3} \left(\frac{g^3}{16\pi^2} \right)$. The vector case is characterized by the presence of soft logs, that can be resummed and therefore needs a different treatment (see Sec. 1.4).

For $b \ll 1/m$, we can cut the integral at some $y = \bar{y} \lesssim O(1)$, obtaining then

$$\hat{F}_1(b^2 \ll 1/m^2) \simeq -\frac{1}{2\pi} \log b/b_{\text{IR}} - \frac{\beta_X}{2\pi g} \log^2(2bm/\bar{y}) . \quad (2.14)$$

Notice that the sign of the quantum corrections is always negative for any value of b and \bar{y} . This will play a major role in the discussion about causality in Sec. 3.

For the helicity flipping contribution, by using the dispersive representation of $F_3(0)$ (see Eq. (1.11)) we can write

$$\hat{F}_3''(b^2) = \frac{i}{8\pi^2 b^4} \int_{2mb}^{+\infty} dy \text{Disc } F_3(y^2/b^2m^2) \left[yK_2(y) - \frac{2}{y} \right] , \quad (2.15)$$

which gets the most important contribution from the region $t \gg m^2$ where the discontinuity converges to a delta function, $\text{Disc } F_3(t \gg m^2) = i\alpha\kappa_X\delta(t)$ for some constant κ_X (see Tab. 2). Therefore, we get

$$\hat{F}_3''(b^2) \simeq -\frac{\alpha\kappa_X}{16\pi^2 b^2} \lim_{y \rightarrow 0} \left[K_2(y) - \frac{2}{y^2} \right] = \frac{\alpha\kappa_X}{32\pi^2 b^2} . \quad (2.16)$$

The full phase shift is then given by

$$\delta_\pm(s, b \ll 1/m) = \delta_0(s, b) - \frac{s\beta_X}{8\pi g m_{\text{Pl}}^2} \log^2 bm/\bar{y} \pm \alpha \frac{s\kappa_X}{8\pi^2 m_{\text{Pl}}^2} , \quad (2.17)$$

where $\kappa_\phi = -1/12$ for a scalar in the loop and $\kappa_\psi = 1/6$ for a fermion. In particular, for small enough impact parameter, the log correction proportional to the β -function will dominate over the constant contribution of $F_3(t)$, as shown numerically in Fig. 4.

Notice, that the change in behavior of the $F_3(t)$ contribution at small impact parameter, from $1/(mb)^2$ to a constant in b , is crucial in the causality discussion. If that was not the case, we would observe causality violation even for the asymptotic definition (see Sec. 3.2). This is avoided thanks to the onset of new physics associated to the particles of mass m before such a violation would become resolvable. We discuss the consequences in Sec. 3.

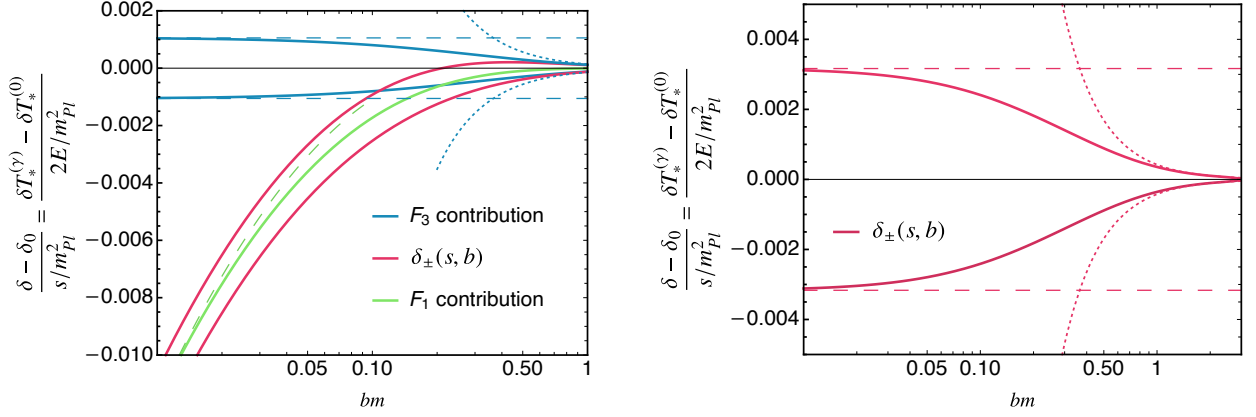


Figure 4: Quantum corrections to the phase shift as function of bm . We plot the full numerical solutions Eq. (2.6) as solid lines, and the limiting behaviors as dotted and dashed lines. On the left the scalar contributions (as discussed, the spinorial case has similar features, so it is not shown here), on the right the vector case. The scalar case has two contributions coming from the form factors $F_3(t)$, relevant at large impact parameters Eq. (2.11), and $F_1(t)$, which dominates as small bm Eq. (2.17). The form factor $F_1(t)$ for vectors is exponentially suppressed by the Sudakov factor, so it does not contribute and the phase shift is dominated by $F_3(t)$ (Eq. (2.18)), which is shown in the plot on the right. The dotted lines for large bm show the EFT result, which if allowed to continue to small bm would eventually give a negative total phase shift and thus time delay. See discussion in Sec. 3.2. We have taken $\bar{y} = 0.27$ to make the approximation close to the exact answer on the scales shown in the plot.

2.2.3 The Small b Limit for Loops of Vectors

The large t behavior of $\text{Disc } F_3(t \gg m^2) = i\alpha\kappa_X\delta(t)$ is still valid for vectors running in the loop, with $\kappa_W = -1/4$. Therefore, the previous argument applies again and the small b limit of the helicity flipping contribution to the phase shift is again given by the constant term in Eq. (2.17).

On the other hand, the contribution of $F_1(t)$ is very different from the scalar and spinorial case. The reason is the resummation of soft infrared divergences, as discussed in section 1.4. In particular, it was shown in Eq. (1.32) that the form factor is exponentially suppressed in the large t regime. This means, that the $F_1(t)$ effects will be subleading, and the phase shift at small b can be safely approximated by

$$\delta_{\pm}(s, b \ll 1/m) = \delta_0(s, b) \pm \alpha \frac{s\kappa_W}{8\pi^2 m_{Pl}^2}. \quad (2.18)$$

3 Causality

In this section we discuss two notions of causality that are both seemingly justified at the classical level, but we show that in fact only one is respected in the quantum theory. Both notions are expressed through the time delay that particles experience relative to the free time evolution in the eikonal scattering.

3.1 Time Delay

We first generalize the time delay relation of [24, 25] to the more general case of non-negligible inelasticity $\text{Im } \delta > 0$, i.e. when other particles can be produced in the scattering.

The idea is to introduce a real parameter δT that labels a family $|f\rangle_{\text{out}}^{\delta T}$ of time delayed 2-particle

states,

$$|f\rangle_{\text{out}}^{\delta T} \equiv \text{Exp}(i\delta TH)|f\rangle_{\text{out}}, \quad |f\rangle_{\text{in/out}} = \int dE \sum_{J,J_z} f_{J,J_z}(E) |E, J, J_z\rangle_{\text{in/out}} \quad (3.1)$$

with normalization ${}_{\text{in}}\langle f|f\rangle_{\text{in}} = {}_{\text{out}}\langle f|f\rangle_{\text{out}} = \int \sum_{J,J_z} dE |f_{J,J_z}(E)|^2 = 1$, and then search for a $\delta T = \delta T_*$ that maximizes the transition probability ${}_{\text{out}}^{\delta T}\langle f|f\rangle_{\text{in}}^2$,

$${}_{\text{out}}^{\delta T}\langle f|f\rangle_{\text{in}} = \int dE \sum_{J,J_z} |f_{J,J_z}(E)|^2 e^{i(2\delta_J(E) - E\delta T)}, \quad (3.2)$$

for some narrowly peaked wave-packet. Here $E = \sqrt{s}$ is the total center of mass energy and J and J_z label the basis where the S -matrix is diagonal. Without spin, J and J_z represent the angular momentum and its projection along the z -axis respectively. Since $|f_{J,J_z}(E)|^2 > 0$, and $\text{Im} \delta_J(E) \geq 0$ by unitarity, the transition probability for a localized wave-packet at $E \simeq E_0$ is maximised at the stationary phase

$$\delta T_* = 2 \frac{\partial \text{Re} \delta_J}{\partial E}(E_0), \quad |{}_{\text{out}}^{\delta T_*}\langle f|f\rangle_{\text{in}}| \simeq e^{-2\text{Im} \delta_J(E_0)} \quad (3.3)$$

where the transition amplitude is less than unity due to the opening of inelastic channels that deplete the elastic amplitude. Notice that Eq. (3.3) reduces to Wigner's formula $\delta T_* = 2 \frac{\partial \delta_J}{\partial E}$ when the phase shift is real. In the eikonal limit of large angular momentum we can replace $\delta_J(E) = \delta(s, b)$, and the notion of time delay becomes

$$\delta T_* = 2 \frac{\partial \text{Re} \delta(s, b)}{\partial E} \quad (3.4)$$

which again reduces to $\delta T_* = 2 \frac{\partial \delta(s, b)}{\partial E}$ for real $\delta(s, b)$.

In the eikonal limit the $|f\rangle_{\text{out}}^{\delta T}$ can be visualised as the family of asymptotic outgoing trajectories emerging from the scattering region and specified by—in addition to the impact parameter and the energy which are preserved in the scattering—the time-shift δT relative to the incoming asymptotic trajectory. The $\delta T = \delta T_*$ corresponds to the emergent semiclassical asymptotic trajectory selected by quantum constructive interference.

The way we derived the time delay makes clear that the asymptotic causality condition $\delta T_* \geq 0$ that we discuss next is meaningful only for δT_* much larger than the quantum mechanical uncertainty $\delta T_{\text{q.m.}} \sim \hbar/E$, which for the $\delta(s, b) \propto s$ in our gravitational setup is just the requirement of large scattering phase shift. Despite such a large phase shift, it is well known that δ remains reliably calculable in the eikonal scattering at large impact parameter against a coherent state of spectators. This is nicely explained in detail in e.g. [2], where the fact that the phase shift grows (at least) linearly with s , which is the case for e.g. Eq. (2.17), (2.18) and (2.11), implies that perturbatively small phases $\tilde{\delta} \ll 1$ of photons scattering against a series of N spectator particles, for $N \gg 1$, exponentiate and add up returning $\delta = N\tilde{\delta} \gg 1$, the phase of scattering against a coherent state.⁸ Scattering against the coherent state can be interpreted to leading order as scattering against a background shock wave at large impact parameter. The connection between scattering in a non-trivial background and causality is reminiscent of the positivity conditions for scattering amplitudes of [1], and the connection to the positivity of time delay has been made explicit in [25].

⁸Alternatively, the exponentiation of the large eikonal phase is reliably calculable when scattering against a particle in the transplanckian regime $t \ll m_{\text{Pl}}^2 \ll s$, see e.g. [22] and references therein, where the theory admits a semiclassical approximation for impact parameters much larger than the Schwarzschild radius $G\sqrt{s}$.

3.2 Asymptotic Causality

By asymptotic causality we mean the following refinement of the Gao-Wald condition [26] used in [2]: the time delay experienced by any particle scattering against (a coherent source of) spectators should be positive

$$\delta T_* \geq 0 \quad (3.5)$$

whenever resolvable and calculable within the range of validity of the theory.

The violation of asymptotic causality would imply that signals sent via massless particles through the bulk of a spacetime perturbed by some spectator field (which could be the graviton itself), would be recorded by a detector at future null infinity at earlier times than if sent instead through an unperturbed empty Minkowski spacetime, which therefore sets the asymptotic causal structure.

Turning the asymptotic causality condition around, forbidding its violation can be used to determine the validity range of the theory, that is putting bounds on the cutoff and/or couplings. For instance, [2] put bounds on the cutoff associated to certain EFTs under the assumption that the higher-dimensional operators are generated at tree level so that the resolution of apparent causality violation should also be resolved at tree level. Tree-level causality bounds are obtained along similar reasoning in e.g. [27–30] and several other works. In this paper we are instead interested in probing the notion of asymptotic causality quantum mechanically.

The results of the previous sections show that this asymptotic notion of causality is in fact respected at one loop in gauge theories that are perturbatively renormalizable before turning on gravity. The reason lies in the change of behavior of the contribution to the phase shift of $F_3(t)$, which transitions from $1/b^2$ in the EFT regime, where charged particles are integrated out, to a constant (see Fig. 4 and Eq. (2.17)), without ever becoming of the size of the leading effect. On the other hand, the $F_1(t)$ contribution, characterized by the sign of the β -function, grows at smaller impact parameters, but the condition $\delta T_* \geq 0$ is always satisfied by the phase shift in Eq. (2.17), as long as the impact parameter b is taken larger than the strong coupling scale b_L of the Landau pole (if any)

$$b > b_L = \frac{1}{m} e^{-g/\beta} \quad \text{for } g/\beta > 0, \quad (3.6)$$

where $\beta > 0$ is the β -function of the gauge coupling g of any spin-0 and spin-1/2 charged particles running in the loop.⁹ The quantum corrections generated by spin-1 particles give instead automatically $\delta T_* \geq 0$ regardless of the impact parameter b (since the $\log b$ in δ_0 of Eq. (2.18) dominates for small impact parameter), consistent with the fact that the non-abelian gauge theory with negative β -function does not need a priori a UV completion before meeting the Planck length $1/m_{\text{Pl}}$.

In other words, within the range of validity of our perturbative calculations, no asymptotic-causality violation is therefore detectable even at the quantum level. Moreover, because of the connection we have established between the sign of the β -function and the sign of the leading quantum corrections to the phase shift $\delta(s, b)$ at small impact parameter, demanding that $\delta T_* \geq 0$ correctly infers the existence of new dynamics at or before the scale of the Landau pole¹⁰ $\Lambda_L = 1/b_L$. That is, either new physics in the form of strong coupling or weakly coupled particles must appear at $b > \max\{b_L, 1/m_{\text{Pl}}\}$.

⁹We also took $mb_{\text{IR}} \gg 1$ while respecting $b_L b_{\text{IR}} m^2 \ll 1$, that is $b_{\text{IR}} < 1/m \text{Exp}(g/\beta)$ which is exponentially larger than $1/m$, hence a valid choice for the IR cutoff for perturbative couplings.

¹⁰In order not to have a trivial bound we are implicitly assuming that the Landau pole of the $U(1)$ gauge theory at hand is smaller than the Planck mass. That is, our analysis applies to theories with α large enough but not too large so that $m \ll \Lambda_L < m_{\text{Pl}}$ is satisfied. For theories with α too small the Landau pole is beyond the Planck mass and the bound trivializes to $b > 1/m_{\text{Pl}}$.

3.3 Bulk Causality

Let's turn now to another notion of causality which stems from the local picture of a lightcone as defined by gravitons traveling through the interior of spacetime. The idea is to race against gravitons through a spacetime perturbed by some spectator field. The bulk (or local) causality condition is the statement that any massless particle would lose the race to the graviton by an amount that is resolvable and calculable within the range of validity of the theory. That is, sending a massless particle and a graviton with the same energy simultaneously through the bulk of a weakly perturbed spacetime, a detector at future null infinity would always record the graviton first and then the other particle.

Sending photons for definiteness, bulk causality implies

$$\delta T_*^{(\gamma)} - \delta T_*^{(0)} \geq 0, \quad (3.7)$$

where $\delta T_*^{(0)} = 2\partial\delta_0(s, b)/\partial E$ is the time delay experienced by gravitons, which is the classic Shapiro time delay. At the classical level the difference in the time delay vanishes, i.e. massless particles travel along the same geodesic, classically, for large impact parameter. The difference in Eq. (3.7) removes the universal term which is also present in the photon time delay as a manifestation of the classical equivalence principle. Therefore, bulk causality Eq. (3.7) is genuinely sensitive to quantum corrections generated by charged states running in the loop.

As a matter of fact, the quantum corrections we calculated in the previous sections violate the bulk-causality condition quantum mechanically, within the range of validity of perturbation theory. Indeed, at small impact parameter for loops of spin-1/2 ($X = \psi$) and spin-0 ($X = \phi$) particles, the difference in time delays is

$$\left(\delta T_*^{(\gamma)} - \delta T_*^{(0)}\right)_X = -\frac{E\beta_X}{4\pi g m_{\text{Pl}}^2} \log^2 bm/\bar{y} \quad (3.8)$$

and is negative for impact parameters much larger than the Landau pole length-scale b_L , see Fig. 4. For spin-1 particles running in the loop, the leading contribution in the same regime is

$$\left(\delta T_*^{(\gamma)} - \delta T_*^{(0)}\right)_W = \pm\alpha \frac{E\kappa_W}{4\pi^2 m_{\text{Pl}}^2} \quad (3.9)$$

which is also negative for some choice of polarization.

All in all, bulk causality is violated at one loop: although light is always slower than gravitons in unperturbed Minkowski space, it can win the race against gravity in a spacetime perturbed by a spectator.¹¹ We interpret this result as evidence against bulk causality, whereas asymptotic causality is respected at one loop.

We emphasize that this conclusion is similar in spirit to the Drummond-Hathrell “paradox” [3] where one is working directly with the velocity of the perturbations in certain backgrounds and charged states have been integrated out. In that case, however, the alleged violation of causality is not resolvable within the validity range of the EFT, see e.g. [31, 32], whereas in our case bulk causality fails within the validity of the perturbative QED theory where the propagating charged particles remain in the spectrum.

We remark also that our analysis is entirely performed within perturbation theory of a renormalizable gauge theory minimally (or conformally) coupled to gravity, i.e. with small coupling $g \ll 1$, large impact parameter $b > \max\{b_L, 1/m_{\text{Pl}}\}$ but possibly $b \ll 1/m$. We have nothing to say about scattering photons outside this domain, in contrast to e.g. [33, 34] that find no bulk-causality violation but, as far as we understand, in a different regime.

¹¹This made the 2020/21 Tokyo Olympics much more challenging for light.

4 Conclusions

Causality is a fundamental concept in classical as well as in quantum physics in flat spacetime, and it is at the core of relativistic QFT. Its implications —its precise incarnation— are however presently not fully understood in gravity, once quantum effects are taken into account in a curved spacetime. Even in the controlled context of AdS-CFT, for example, it is still not completely clear whether it is the dynamical light-cone in the bulk or the one on the boundary that determines the causality condition, see e.g. [35].

In this work we have studied causality in gravity to the first post-Minkowskian order around flat spacetime, focusing on the leading quantum effects in a gauge theory. We have in particular contrasted two notions of causality —“asymptotic” and “bulk” causality— in a gauge theory where both are respected in the classical limit, but differ quantum mechanically.

The causal and quantum response of photons to a weak spacetime perturbation is captured by the photon energy-momentum tensor that we have calculated by exploiting unitarity cuts and on-shell techniques, determining the one-loop form factors generated by charged scalars, spinors, and vectors running in the loop. In analogy to the electroweak currents, vector loops give rise to large IR Sudakov log-factors in the energy-momentum tensor, that we have re-summed.

We have studied the eikonal phase shift of photons scattering against (a coherent source of) spectator particles responsible for bending the spacetime. In the limit of large impact parameter, the theory is well approximated by an EFT with higher dimensional operators, and we have reproduced the classic result of [2] and its implication for causality. In particular, the would-be violation of asymptotic causality in the EFT can be used to determine the shortest impact parameter where the EFT must necessarily break down, to be replaced by a new theory where microscopic degrees of freedom (the charged state and possibly Higgs bosons) are integrated-in.

Beyond the large impact-parameter limit, and studying the time delay all the way down to the Landau-pole scale, we have explicitly established how asymptotic causality is actually respected in the gauge theory coupled to gravity. The helicity-flipping form factor that would have led to causality violation in the EFT changes behavior as the impact parameter becomes comparable to the Compton wavelength of the particles running in the loop. It transitions to a constant value, subleading to the helicity-preserving form factor which becomes instead the leading correction to the classic Shapiro time delay. Moreover, the sign correction to the time delay, at small impact parameter, is opposite to the sign of the β -function generated by the particles in the loop.

We have found that asymptotic causality, i.e. positivity of the time delay relative to a photon travelling in unperturbed flat spacetime, is therefore respected up to the scale of the Landau pole (if any), where the perturbative regime breaks down and our calculation is no longer valid. Conversely, the presence of the Landau pole can be correctly inferred by demanding asymptotic causality in a gravitational scattering. For theories with a negative β -function, asymptotic causality holds up to the Planck length.

The fate of bulk causality, that is the notion that photons should travel locally slower (or at the same speed) than gravitons in the bulk of same spacetime, is different. Bulk causality implies that the difference between photon and graviton time delays should be non-negative, which is respected classically. We have found instead that quantum-mechanically (some polarization of) photons always display a smaller time delay than gravitons, representing a violation of bulk causality at the quantum level.

Looking at future directions, it would be interesting to understand the implication of bulk-causality violation or, perhaps, how to recover it and why. In particular, it would be interesting to include

next orders in the post-Minkowskian expansion in $1/m_{\text{Pl}}^2$ in the photon and graviton time delays, and compare the competing contributions between the gauge and gravitational couplings. We find intriguing the possibility of turning bulk causality into a statement about the swampland versus the landscape in gravitational theories, in analogy to the Weak-Gravity Conjecture [36]. Going to higher orders in the post-Minkowskian expansion is also interesting in itself because of extra IR divergences, other than the ones we re-summed in this work, that can arise from loops and real emissions involving gravitons, see e.g. [37]. Understanding IR divergences in gravity and extracting physical observables and well defined S -matrix elements is a long-standing research program which has recently become phenomenologically even more relevant because of its connection to the gravitational waves emitted in black hole and/or neutron star mergers.

Finally, while we focused in this work on the quantum corrections to the 3-point function and their implications for causality in gravity, there has been recent progress in understanding how causality and unitarity are imprinted in the analytic structure and positivity of 4-point functions [38, 39]. It would be extremely interesting to study causality via 4-point functions including the IR quantum effects from loops of massless states.

Acknowledgments

We thank Sasha Zhiboedov and Herman Verlinde for useful discussions. We thank Javi Serra for the continuous discussions, insights, and advice throughout this work, and his early participation. F.S. is supported by a Klarman Fellowship at Cornell University, and also supported in part by the NSF grant PHY-2014071. M.L. acknowledges the Northwestern University Amplitudes and Insight group, Department of Physics and Astronomy, and Weinberg College, and is also supported by the DOE under contract DE-SC0021485.

A Conventions

We are working in the mostly minus signature convention $\eta_{\mu\nu} = \text{diag}(+, -, -, -)$, with Riemann tensor $R^\mu_{\nu\rho\sigma} = \partial_\rho \Gamma^\mu_{\sigma\nu} + \dots$, Ricci tensor $R_{\nu\sigma} = R^\mu_{\nu\mu\sigma}$, Weyl tensor $W^{\mu\nu\rho\sigma} = R^{\mu\nu\rho\sigma} - \text{traces}$. Symmetrization and antisymmetrization does not involve factorials, e.g. $A_{[ab]} = A_{ab} - A_{ba}$ and $A_{(ab)} = A_{ab} + A_{ba}$. The discontinuity across the real line of an analytic function $F(t)$ in the cut t -plane is defined as $\text{Disc } F(t) = F(t + i\epsilon) - F(t - i\epsilon)$. The one particle states are normalized relativistically, $\langle k'^h | k^h \rangle = \delta^{hh'} (2\pi)^3 \delta^{(3)}(\mathbf{k} - \mathbf{k}') 2\sqrt{\mathbf{k}^2 + m^2}$, where \mathbf{k} is a three-dimensional vector.

We work with the following spinor conventions. The momentum k_i of a massless particle i is rewritten as

$$(k_i \sigma)_{\alpha\dot{\beta}} = \lambda_{i\alpha} \tilde{\lambda}_{i\dot{\beta}}, \quad (\text{A.1})$$

where $[\sigma^\mu]_{\alpha\dot{\beta}} = (1, \vec{\sigma})$. The objects λ_i and $\tilde{\lambda}_i$ are respectively holomorphic and anti-holomorphic spinors, transforming as $\lambda_i \rightarrow t_i^{-1} \lambda_i$, $\tilde{\lambda}_i \rightarrow t_i \tilde{\lambda}_i$ under a $U(1)$ little group transformation. The spinor-helicity angle (square) brackets with positive energy correspond to negative (positive) 1/2-helicities.

A similar construction is done for massive momenta [6]

$$(k_i \sigma)_{\alpha\dot{\beta}} = \sum_{J=1}^2 \chi_i^J \tilde{\chi}_{i\dot{\beta}J}, \quad (\text{A.2})$$

where the $J = 1, 2$ index is associated with the $SU(2)$ little group. For each external state, a full symmetrization of these indices is necessary to reproduce different polarizations. For clarity, the J

index as well as the symmetrization is kept implicit in the main text.

Lorentz-invariant spinor contractions are abbreviated using the bra-ket notation. For massless spinors

$$\langle ij \rangle \equiv \lambda_i^\alpha \lambda_{j\alpha} = \epsilon^{\beta\alpha} \lambda_{i\alpha} \lambda_{j\beta}, \quad [ij] \equiv \tilde{\lambda}_{i\dot{\alpha}} \tilde{\lambda}_{j\dot{\alpha}} = \epsilon^{\dot{\alpha}\dot{\beta}} \tilde{\lambda}_{i\dot{\alpha}} \tilde{\lambda}_{j\dot{\beta}}, \quad (\text{A.3})$$

where ϵ is the anti-symmetric tensor. We use the notation $\langle ip_k j \rangle \equiv \lambda_i p_k \sigma \tilde{\lambda}_j = \langle ik \rangle [kj]$. Similarly, for massive spinors

$$\langle \mathbf{ij} \rangle \equiv \epsilon^{\beta\alpha} \chi_{i\alpha}^J \chi_{j\beta}^K, \quad [\mathbf{ij}] \equiv \epsilon^{\dot{\alpha}\dot{\beta}} \tilde{\chi}_{i\dot{\alpha}}^J \tilde{\chi}_{j\dot{\beta}}^K. \quad (\text{A.4})$$

The **bold** notation allows to differentiate between massive and massless states. Finally, the Mandelstam variables are given by

$$s_{ij} = (k_i + k_j)^2 = \langle ij \rangle [ji]. \quad (\text{A.5})$$

B Free Energy-Momentum Tensors

The free energy-momentum tensor for photons γ , a minimally coupled massless neutral (scalar) spectators S , and charged spinning particles with $J \leq 1$

$$\begin{aligned} T_{\mu\nu}^{(\gamma)} &= -F_{\mu\alpha} F_\nu^\alpha + \frac{1}{4} \eta_{\mu\nu} (F_{\alpha\beta} F^{\alpha\beta}) \\ T_{\mu\nu}^{(S)} &= \partial_\mu S \partial_\nu S - \frac{\eta_{\mu\nu}}{2} (\partial S)^2 \\ T_{\mu\nu}^{(J=0)}(x) &= \partial_\mu \phi^\dagger \partial_\nu \phi + \partial_\mu \phi \partial_\nu \phi^\dagger - \eta_{\mu\nu} (|\partial\phi|^2 - m^2 |\phi|^2) - \frac{\xi}{3} (\partial_\mu \partial_\nu - \eta_{\mu\nu} \square) |\phi|^2 \\ T_{\mu\nu}^{(J=1/2)} &= \frac{1}{4} \bar{\psi} \gamma_{(\mu} i \overleftrightarrow{\partial}_{\nu)} \psi - \eta_{\mu\nu} \bar{\psi} (i \frac{\overleftrightarrow{\not{\partial}}}{2} - m) \psi \\ T_{\mu\nu}^{(J=1)}(x) &= -W_{\mu\alpha}^\dagger W_\nu^\alpha - W_{\mu\alpha} W_\nu^{\dagger\alpha} + \frac{1}{2} g_{\mu\nu} (W_{\alpha\beta}^\dagger W^{\alpha\beta}) + m_W^2 (W_\mu^\dagger W_\nu + W_\mu W_\nu^\dagger) - m_W^2 \eta_{\mu\nu} W_\alpha^\dagger W^\alpha, \end{aligned} \quad (\text{B.1})$$

sum up to the total free energy-momentum tensor $T_{\mu\nu}(x) = T_{\mu\nu}^{(\gamma)}(x) + T_{\mu\nu}^{(S)}(x) + \sum_{J \leq 1} T_{\mu\nu}^{(J)}(x)$. The scalar contribution $T_{\mu\nu}^{(J=0)}(x)$ is defined only up to an improvement term controlled by ξ . It can be derived from the action $\int d^4x \sqrt{-g} \left\{ |\partial\phi|^2 - m^2 |\phi|^2 + \frac{\xi}{6} |\phi|^2 R \right\}$ via $\int d^4x \sqrt{-g} \frac{1}{2} T_{\mu\nu} \delta g^{\mu\nu} = \delta S$, where $\xi = 0$ corresponds to a minimally coupled scalar whereas for $\xi = 1$ the scalar is conformally coupled, the action being classically scale invariant when $m = 0$. At the quantum level the $T_{\mu\nu}$ does not mix with other conserved operators for $\xi = 1$. For the scalar spectator field we chose $\xi = 0$ for simplicity. The phase shift in the eikonal limit is insensitive to the F_2 form factors and it is therefore independent of ξ .

C Higgs/Graviton Mixing

In this appendix we show that Eq. (1.14), which is the non-trivial Higgs boson contribution to the scattering of photons against spectators —neither of which naïvely couples to the Higgs— can be phrased in terms of Higgs/graviton mixing. After resolving the mixing the Higgs couples to all fields with non-vanishing energy-momentum trace.

The the 3pt vertex $-h_{\mu\nu}T^{\mu\nu}/m_{\text{Pl}}$ between gravitons and Higgs generates indeed a kinetic mixing after shifting field around the VEV

$$-h_{\mu\nu}\delta T_{\mu\nu}/m_{\text{Pl}} = \left(\frac{v\xi_H}{3m_{\text{Pl}}}\right) h_{\mu\nu} (\partial_\mu\partial_\nu - \eta_{\mu\nu}\square) H + \dots \quad (\text{C.1})$$

The mixing is removed at the linear order by the field redefinition (a linearized Weyl transformation) $h_{\mu\nu} \rightarrow h_{\mu\nu} + \eta_{\mu\nu}H \left(\frac{v\xi_H}{6m_{\text{Pl}}}\right)$ as one can check following the transformation of the graviton kinetic term, namely $-2h_{\mu\nu}(\partial_\mu\partial_\nu - \eta_{\mu\nu}\square)H \left(\frac{v\xi_H}{6m_{\text{Pl}}}\right)$. The transformation generates as well a coupling between the Higgs and any particle the graviton was coupling to, in particular to the trace $T_\mu^{\mu(S)} = -(\partial S)^2$ of the massless spectators S , namely

$$-\frac{1}{m_{\text{Pl}}}h^{\mu\nu}T_{\mu\nu}^{(S)} \rightarrow -\frac{1}{m_{\text{Pl}}}\left(\frac{v\xi_H}{6m_{\text{Pl}}}\right)T_\mu^{\mu(S)}H \quad (\text{C.2})$$

so that the scattering of photons with spectators receives a contribution at one-loop by the Higgs boson exchange as reported in Eq. (1.14).

D Explicit Form Factors at One Loop

In this appendix we summarize the full results of the loop calculations both for the discontinuities of $F_2(t)$ and $F_3(t)$ for the full form factors integrated by dispersion relations (1.11). In the following $\tau = 1 - 4m^2/t$.

In the case of fermion loops, we find perfect agreement with the results of [7, 40]. Comparing our results with Ref. [41, 42] that discuss spin-1 and Higgs contributions we find excellent but not perfect agreement. A small discrepancy is found for the F_1 form factor: rather than $[5m_W^2 + 7s]$ in front to $-1/2D_0$ in the first line of Eq. (149) of Ref. [41], we have $[5m_W^2 + \frac{7}{2}s]$. This discrepancy corresponds to a difference in the imaginary parts by an amount $\text{Disc } \delta F_1 = \frac{7}{2}i\alpha\sqrt{1 - \frac{4m_W^2}{s_{13}}}$. It's very remarkable that the contribution of tens of diagrams in [41] is reproduced in the present work by integrating the discontinuity of just one or two diagrams.

Electron loops

$$\text{Disc } F_1(t) = \frac{2i\alpha}{3t^2} \left(\sqrt{\tau} (5m^2 + t) t - 6m^2 (2m^2 + t) \tanh^{-1} \sqrt{\tau} \right) \theta(t - 4m^2) \quad (\text{D.1a})$$

$$\text{Disc } F_2(t) = i \frac{2\alpha m^2}{t^3} \left(t\sqrt{\tau} - 4m^2 \tanh^{-1} \sqrt{\tau} \right) \theta(t - 4m^2) \quad (\text{D.1b})$$

$$\text{Disc } F_3(t) = i \frac{2\alpha m^2}{t^3} \left(-3t\sqrt{\tau} + 2(2m^2 + t) \tanh^{-1} \sqrt{\tau} \right) \theta(t - 4m^2). \quad (\text{D.1c})$$

$$F_1(t) = 1 + \frac{\alpha}{\pi} \left[-\frac{13\tau}{12} + \frac{3}{16} \log^2 \left(1 - \frac{2}{\sqrt{\tau}+1} \right) + \frac{37}{18} + \frac{\tau-4}{4} \tau (\coth^{-1} \sqrt{\tau})^2 + \frac{5\tau-9}{6} \sqrt{\tau} \coth^{-1} \sqrt{\tau} \right] \quad (\text{D.1d})$$

$$F_2(t) = \frac{\alpha}{\pi} \left[\frac{(\tau-1)}{192m^2} \left(36\tau - 3 \log^2 \left(1 - \frac{2}{\sqrt{\tau}+1} \right) - 32 \right) - \frac{\sqrt{\tau}(\tau-1)^2}{8m^2} \coth^{-1} \sqrt{\tau} - \frac{(\tau-2)\tau(\tau-1)}{16m^2} (\coth^{-1} \sqrt{\tau})^2 \right] \quad (\text{D.1e})$$

$$F_3(t) = \frac{\alpha}{\pi} \left\{ (\tau-1) \left(-\frac{7\tau}{16m^2} + \frac{3 \log^2 \left(1 - \frac{2}{\sqrt{\tau}+1} \right)}{64m^2} + \frac{11}{24m^2} \right) + \frac{3\sqrt{\tau}(\tau-1)^2 \coth^{-1} \sqrt{\tau}}{8m^2} + \frac{(\tau-4)\tau(\tau-1) (\coth^{-1} \sqrt{\tau})^2}{16m^2} \right\} \quad (\text{D.1f})$$

Scalar loops

$$\text{Disc } F_1(t) = \frac{i\alpha}{6t^2} (t(t-10m^2) \sqrt{\tau} + 24m^4 \tanh^{-1} \sqrt{\tau}) \theta(t-4m^2) \quad (\text{D.2a})$$

$$\text{Disc } F_2(t) = \frac{i\alpha}{t^3} m^2 (-t\sqrt{\tau} + 2(2m^2+t) \tanh^{-1} \sqrt{\tau}) \theta(t-4m^2) - \frac{4i\alpha m^2 \xi_\phi \tanh^{-1} \sqrt{\tau}}{3t^2} \theta(t-4m^2) \quad (\text{D.2b})$$

$$\text{Disc } F_3(t) = \frac{i\alpha m^2}{t^3} (3t\sqrt{\tau} - 2(2m^2+t) \tanh^{-1} \sqrt{\tau}) \theta(t-4m^2) \quad (\text{D.2c})$$

$$F_1(t) = 1 + \frac{\alpha}{8\pi t} \left[-\frac{1}{4} t \log^2 \left(\frac{\sqrt{\tau}-1}{\sqrt{\tau}+1} \right) + \left(t - \frac{16m^4}{t} \right) (\coth^{-1} \sqrt{\tau})^2 - \frac{4}{3} \sqrt{\tau} (t-10m^2) \coth^{-1} \sqrt{\tau} - \frac{52m^2}{3} + \frac{19t}{9} \right] \quad (\text{D.2d})$$

$$F_2(t) = -\frac{5\alpha}{24\pi t} \left[1 + \frac{\tau((4\xi_\phi-9)t-12m^2)}{5t} (\coth^{-1} \sqrt{\tau})^2 + \frac{1}{20} (9-4\xi_\phi) \log^2 \left(\frac{\sqrt{\tau}-1}{\sqrt{\tau}+1} \right) + \frac{36m^2}{5t} - \frac{24m^2 \sqrt{\tau}}{5t} \coth^{-1} \sqrt{\tau} - \frac{4\xi_\phi}{5} \right] \quad (\text{D.2e})$$

$$F_3(t) = \frac{\alpha}{24\pi t} \left[1 + \left(\frac{48m^4}{t^2} + \frac{24m^2}{t} - 9 \right) (\coth^{-1} \sqrt{\tau})^2 + \frac{84m^2}{t} + \frac{9}{4} \log^2 \left(\frac{\sqrt{\tau}-1}{\sqrt{\tau}+1} \right) - \frac{72m^2 \sqrt{\tau}}{t} \coth^{-1} \sqrt{\tau} \right] \quad (\text{D.2f})$$

Vector loops

$$\text{Disc } F_1(t) = \frac{-i\alpha}{2t^2} (t\sqrt{\tau} (10m^2 + 7t) - 8(m^2 + t)(3m^2 + t) \tanh^{-1} \sqrt{\tau}) \theta(t - 4m^2) \quad (\text{D.3a})$$

$$\text{Disc } F_2(t) = -\frac{i\alpha m^2}{t^3} (3t\sqrt{\tau} + 2(t - 6m^2) \tanh^{-1} \sqrt{\tau}) \theta(t - 4m^2) \quad (\text{D.3b})$$

$$\text{Disc } F_3(t) = -\frac{3i\alpha m^2}{t^3} (-3t\sqrt{\tau} + 2(2m^2 + t) \tanh^{-1} \sqrt{\tau}) \theta(t - 4m^2) \quad (\text{D.3c})$$

$$F_1(t) = 1 - \frac{\alpha}{2\pi t} \left[\frac{35}{16} t \log^2 \frac{\sqrt{\tau} - 1}{\sqrt{\tau} + 1} + \left(\frac{12m^4}{t} + 16m^2 - \frac{19t}{4} \right) (\coth^{-1} \sqrt{\tau})^2 - \sqrt{\tau} (10m^2 + 7t) \coth^{-1} \sqrt{\tau} + 13m^2 + \frac{125t}{12} \right] \quad (\text{D.3d})$$

$$F_2(t) = -\frac{\alpha}{8\pi t} \left[-\frac{\tau (12m^2 + t)}{t} (\coth^{-1} \sqrt{\tau})^2 + \frac{36m^2}{t} + \frac{1}{4} \log^2 \frac{\sqrt{\tau} - 1}{\sqrt{\tau} + 1} - \frac{24m^2 \sqrt{\tau}}{t} \coth^{-1} (\sqrt{\tau}) - 3 \right] \quad (\text{D.3e})$$

$$F_3(t) = -\frac{\alpha}{\pi t} \left[\left(-\frac{6m^4}{t^2} - \frac{3m^2}{t} + \frac{9}{8} \right) (\coth^{-1} \sqrt{\tau})^2 - \frac{84m^2 + t}{8t} - \frac{9}{32} \log^2 \frac{\sqrt{\tau} - 1}{\sqrt{\tau} + 1} + \frac{9m^2 \sqrt{\tau}}{t} \coth^{-1} (\sqrt{\tau}) \right] \quad (\text{D.3f})$$

Higgs boson contribution

The models dependent Higgs boson contribution can be found in Eq. (1.17) that for a Higgs coupled to unit-charge spin-1 boson gives Eq. (1.20).

E Off-Shell Vertices

All amplitudes presented in this paper can be recovered by Feynman diagrams starting from the following Lagrangians. For scalars, the coupling to the gauge field is given by the covariant kinetic term $|D_\mu \phi|^2$, which expanded leads to

$$\mathcal{L}^{J=0} = |\partial_\mu \phi|^2 - m^2 |\phi|^2 - ig(\partial_\mu \phi^+ \phi^- - \phi^+ \partial_\mu \phi^-) A^\mu + g^2 A_\mu A^\mu |\phi|^2. \quad (\text{E.1})$$

In the same way the Lagrangian of spinors and massive vectors coupled to the gauge field are given by

$$\mathcal{L}^{J=1/2} = i\bar{\psi} \gamma^\mu \partial_\mu \psi - m\bar{\psi} \psi - g\bar{\psi} \gamma^\mu A_\mu \psi, \quad (\text{E.2})$$

$$\begin{aligned} \mathcal{L}^{J=1} = & -\frac{1}{2} W_{\mu\nu}^\dagger W^{\mu\nu} + m_W^2 W_\mu^\dagger W^\mu \\ & + ig F_{\mu\nu} W_\mu W_\nu^\dagger - ig A_\mu (W_{\mu\nu} W_\nu^\dagger - W_{\mu\nu}^\dagger W_\nu) - g^2 (A_\mu^2 |W_\nu|^2 - |A_\mu W^\mu|^2). \end{aligned} \quad (\text{E.3})$$

Additionally to the trilinear coupling of photons to the $U(1)$ global current there is also a non-minimal trilinear coupling $F_{\mu\nu} W_\mu W_\nu^\dagger$ with a tuned coefficient (as set by embedding it in a non-abelian theory) required to produce the gyromagnetic factor value of 2.

References

- [1] A. Adams, N. Arkani-Hamed, S. Dubovsky, A. Nicolis, and R. Rattazzi, “Causality, Analyticity and an IR Obstruction to UV Completion,” *JHEP* **10** (2006) 014, [hep-th/0602178](#).
- [2] X. O. Camanho, J. D. Edelstein, J. Maldacena, and A. Zhiboedov, “Causality Constraints on Corrections to the Graviton Three-Point Coupling,” *JHEP* **02** (2016) 020, [1407.5597](#).
- [3] I. T. Drummond and S. J. Hathrell, “Qed Vacuum Polarization in a Background Gravitational Field and Its Effect on the Velocity of Photons,” *Phys. Rev.* **D22** (1980) 343.
- [4] C. Cheung, “TASI Lectures on Scattering Amplitudes,” in *Proceedings, Theoretical Advanced Study Institute in Elementary Particle Physics : Anticipating the Next Discoveries in Particle Physics (Tasi 2016): Boulder, Co, Usa, June 6-July 1, 2016*, pp. 571–623, 2018. [1708.03872](#).
- [5] H. Elvang and Y.-t. Huang, “Scattering Amplitudes,” [1308.1697](#).
- [6] N. Arkani-Hamed, T.-C. Huang, and Y.-t. Huang, “Scattering Amplitudes for All Masses and Spins,” [1709.04891](#).
- [7] F. A. Berends and R. Gastmans, “Quantum Electrodynamical Corrections to Graviton-Matter Vertices,” *Annals Phys.* **98** (1976) 225.
- [8] C. Cheung and G. N. Remmen, “Infrared Consistency and the Weak Gravity Conjecture,” *JHEP* **12** (2014) 087, [1407.7865](#).
- [9] M. S. Chanowitz and M. K. Gaillard, “The TeV Physics of Strongly Interacting W’s and Z’s,” *Nucl. Phys. B* **261** (1985) 379–431.
- [10] J. Horejsi, “Electroweak Interactions and High-Energy Limit: an Introduction to Equivalence Theorem,” *Czech. J. Phys.* **47** (1997) 951–977, [hep-ph/9603321](#).
- [11] M. A. Shifman, A. I. Vainshtein, M. B. Voloshin, and V. I. Zakharov, “Low-Energy Theorems for Higgs Boson Couplings to Photons,” *Sov. J. Nucl. Phys.* **30** (1979) 711–716.
- [12] K. Melnikov and A. Vainshtein, “Higgs Boson Decay to Two Photons and Dispersion Relations,” *Phys. Rev. D* **93** (2016), no. 5 053015, [1601.00406](#).
- [13] S. Caron-Huot and M. Wilhelm, “Renormalization Group Coefficients and the S-Matrix,” *JHEP* **12** (2016) 010, [1607.06448](#).
- [14] A. D. Dolgov and V. I. Zakharov, “On Conservation of the Axial Current in Massless Electrodynamics,” *Nucl. Phys. B* **27** (1971) 525–540.
- [15] S. R. Coleman and B. Grossman, “’t Hooft’s Consistency Condition as a Consequence of Analyticity and Unitarity,” *Nucl. Phys. B* **203** (1982) 205–220.
- [16] M. Giannotti and E. Mottola, “The Trace Anomaly and Massless Scalar Degrees of Freedom in Gravity,” *Phys. Rev. D* **79** (2009) 045014, [0812.0351](#).
- [17] P. Ciafaloni and D. Comelli, “Sudakov Enhancement of Electroweak Corrections,” *Phys. Lett. B* **446** (1999) 278–284, [hep-ph/9809321](#).

- [18] V. S. Fadin, L. N. Lipatov, A. D. Martin, and M. Melles, “Resummation of Double Logarithms in Electroweak High-Energy Processes,” *Phys. Rev. D* **61** (2000) 094002, [hep-ph/9910338](#).
- [19] M. Ciafaloni, P. Ciafaloni, and D. Comelli, “Anomalous Sudakov Form Factors,” *JHEP* **03** (2010) 072, [0909.1657](#).
- [20] D. Amati, M. Ciafaloni, and G. Veneziano, “Classical and Quantum Gravity Effects from Planckian Energy Superstring Collisions,” *Int. J. Mod. Phys. A* **3** (1988) 1615–1661.
- [21] D. Amati, M. Ciafaloni, and G. Veneziano, “Planckian Scattering Beyond the Semiclassical Approximation,” *Phys. Lett. B* **289** (1992) 87–91.
- [22] D. N. Kabat and M. Ortiz, “Eikonal Quantum Gravity and Planckian Scattering,” *Nucl. Phys. B* **388** (1992) 570–592, [hep-th/9203082](#).
- [23] M. Accettulli Huber, A. Brandhuber, S. De Angelis, and G. Travaglini, “Eikonal Phase Matrix, Deflection Angle and Time Delay in Effective Field Theories of Gravity,” *Phys. Rev. D* **102** (2020), no. 4 046014, [2006.02375](#).
- [24] L. Maiani and M. Testa, “Unstable systems in relativistic quantum field theory,” *Annals Phys.* **263** (1998) 353–367, [hep-th/9709110](#).
- [25] N. Arkani-Hamed, T.-C. Huang, and Y.-T. Huang, “The EFT-Hedron,” [2012.15849](#).
- [26] S. Gao and R. M. Wald, “Theorems on Gravitational Time Delay and Related Issues,” *Class. Quant. Grav.* **17** (2000) 4999–5008, [gr-qc/0007021](#).
- [27] K. Hinterbichler, A. Joyce, and R. A. Rosen, “Massive Spin-2 Scattering and Asymptotic Superluminality,” *JHEP* **03** (2018) 051, [1708.05716](#).
- [28] J. Bonifacio, K. Hinterbichler, A. Joyce, and R. A. Rosen, “Massive and Massless Spin-2 Scattering and Asymptotic Superluminality,” *JHEP* **06** (2018) 075, [1712.10020](#).
- [29] N. Afkhami-Jeddi, S. Kundu, and A. Tajdini, “A Bound on Massive Higher Spin Particles,” *JHEP* **04** (2019) 056, [1811.01952](#).
- [30] J. Kaplan and S. Kundu, “A Species or Weak-Gravity Bound for Large N Gauge Theories Coupled to Gravity,” *JHEP* **11** (2019) 142, [1904.09294](#).
- [31] G. Goon and K. Hinterbichler, “Superluminality, Black Holes and EFT,” *JHEP* **02** (2017) 134, [1609.00723](#).
- [32] C. de Rham and A. J. Tolley, “Causality in Curved Spacetimes: the Speed of Light and Gravity,” *Phys. Rev. D* **102** (2020), no. 8 084048, [2007.01847](#).
- [33] T. J. Hollowood and G. M. Shore, “Causality Violation, Gravitational Shockwaves and UV Completion,” *JHEP* **03** (2016) 129, [1512.04952](#).
- [34] T. J. Hollowood and G. M. Shore, “Causality, Renormalizability and Ultra-High Energy Gravitational Scattering,” *J. Phys. A* **49** (2016), no. 21 215401, [1601.06989](#).
- [35] L. McGough, M. Mezei, and H. Verlinde, “Moving the CFT into the bulk with $T\bar{T}$,” *JHEP* **04** (2018) 010, [1611.03470](#).

- [36] N. Arkani-Hamed, L. Motl, A. Nicolis, and C. Vafa, “The String Landscape, Black Holes and Gravity as the Weakest Force,” *JHEP* **06** (2007) 060, [hep-th/0601001](#).
- [37] M. Ciafaloni, D. Colferai, and G. Veneziano, “Infrared Features of Gravitational Scattering and Radiation in the Eikonal Approach,” *Phys. Rev. D* **99** (2019), no. 6 066008, [1812.08137](#).
- [38] S. Caron-Huot, D. Mazac, L. Rastelli, and D. Simmons-Duffin, “Sharp Boundaries for the Swampland,” [2102.08951](#).
- [39] Z. Bern, D. Kosmopoulos, and A. Zhiboedov, “Gravitational Effective Field Theory Islands, Low-Spin Dominance, and the Four-Graviton Amplitude,” [2103.12728](#).
- [40] K. A. Milton, “Quantum Electrodynmic Corrections to the Gravitational Interaction of the Photon,” *Phys. Rev. D* **15** (1977) 2149–2155.
- [41] C. Coriano, L. Delle Rose, and M. Serino, “Gravity and the Neutral Currents: Effective Interactions from the Trace Anomaly,” *Phys. Rev. D* **83** (2011) 125028, [1102.4558](#).
- [42] R. Armillis, C. Coriano, and L. Delle Rose, “Trace Anomaly, Massless Scalars and the Gravitational Coupling of QCD,” *Phys. Rev. D* **82** (2010) 064023, [1005.4173](#).